
MODEL GENERALIZATION ON TEXT ATTRIBUTE GRAPHS: PRINCIPLES WITH LARGE LANGUAGE MODELS

Haoyu Wang	Shikun Liu	Rongzhe Wei	Pan Li
Department of ECE	Department of ECE	Department of ECE	Department of ECE
Georgia Tech	Georgia Tech	Georgia Tech	Georgia Tech
haoyu.wang@gatech.edu	shikun.liu@gatech.edu	rongzhe.wei@gatech.edu	panli@gatech.edu

ABSTRACT

Large language models (LLMs) have recently been introduced to graph learning, aiming to extend their zero-shot generalization success to tasks where labeled graph data is scarce. Among these applications, inference over text-attributed graphs (TAGs) presents unique challenges: existing methods struggle with LLMs’ limited context length for processing large node neighborhoods and the misalignment between node embeddings and the LLM token space. To address these issues, we establish two key principles for ensuring generalization and derive the framework LLM-BP accordingly: (1) **Unifying the attribute space with task-adaptive embeddings**, where we leverage LLM-based encoders and task-aware prompting to enhance generalization of the text attribute embeddings; (2) **Developing a generalizable graph information aggregation mechanism**, for which we adopt belief propagation with LLM-estimated parameters that adapt across graphs. Evaluations on 11 real-world TAG benchmarks demonstrate that LLM-BP significantly outperforms existing approaches, achieving 8.10% improvement with task-conditional embeddings and an additional 1.71% gain from adaptive aggregation. Task-adaptive embeddings and codes are publicly available at¹.

1 Introduction

Inspired by the remarkable generalization capabilities of foundation models for text and image data [1, 2, 3], researchers have recently explored extending these successes to graph data [4, 5, 6, 7, 8], aiming to develop models that generalize to new or unseen graphs and thereby reduce reliance on costly human annotation [9, 10, 11, 12]. Among various types of graph data, *text-attributed graphs* (TAGs) have found a wide range of applications. These graphs combine both topological relationships and textual attributes associated with each node, which naturally arises in recommendation systems (where user and item nodes may have textual descriptions or reviews) [13], academic graphs (where publications include extensive textual metadata) [14, 15], and financial networks (where transactions and accounts come with textual records) [16, 17]. Given the labeling challenges posed by cold-start problems in recommendation systems or fraud detection in financial networks, methods that can operate with limited labeled data are crucial. In particular, robust zero-shot node labeling across unseen TAGs has become an area of great interest.

Numerous studies have been dedicated to inference tasks on TAGs. Early efforts have primarily focused on adapting pre-trained language model (LM) encoders [18, 19], sometimes in combination with graph neural networks (GNNs) [20, 21], to incorporate structural information. However, these approaches often struggle to achieve strong generalization performance, largely due to the limited capacity of the underlying models. With the advent of large language models (LLMs) [22, 23], researchers have proposed two main strategies for integrating LLMs into TAG inference: 1) **Direct Node-Text Input**. Here, raw node texts are directly fed into LLMs. This method demonstrates reasonably good zero-shot performance on TAGs when text attributes are highly informative for node labels [24, 25]. However, when the textual attributes are insufficient, it becomes necessary to aggregate information from a larger neighborhood in the graph, while this is constrained by the limited context length LLMs can digest and reason over. 2) **Embedding-Based Integration**. In this approach, node texts and their neighboring structural information are first encoded into compressed

¹ https://github.com/Graph-COM/LLM_BP,
<https://huggingface.co/datasets/Graph-COM/Text-Attributed-Graphs>

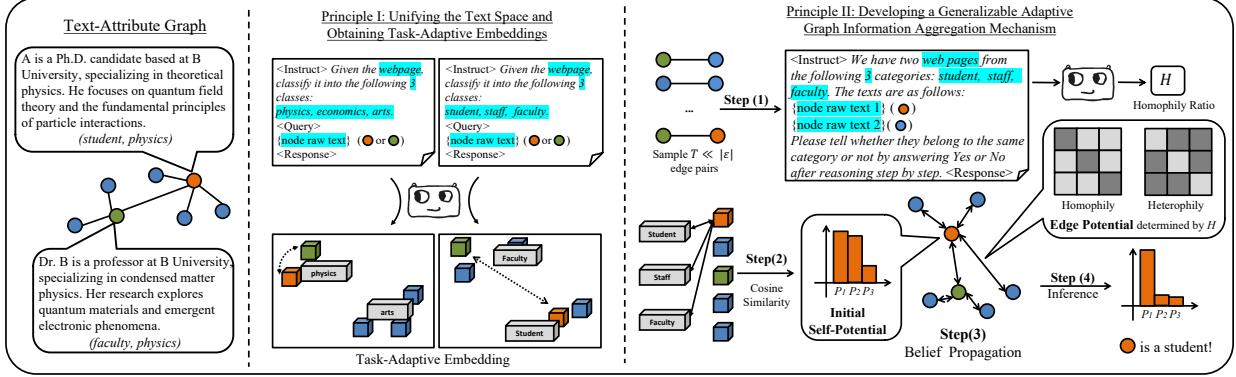


Figure 1: The two generalization principles and the framework of LLM-BP.

embeddings, which are then processed by LLMs [26, 27, 28, 29, 30]. Because LLMs are not inherently trained on arbitrary embedding spaces, aligning these embeddings with the LLM’s token space is essential - an idea partly inspired by how vision-language models align multimodal data [3, 31]. However, unlike the vision-language domain, where large-scale text-image pairs [32] are abundant, the graph domain typically lacks comparable datasets. This scarcity reduces the model’s generalization in practice.

In contrast to prior heuristic approaches, this work aims to design a method from first principles for robust zero-shot generalization on TAGs. Because TAGs are inherently multimodal, the proposed method must simultaneously address potential distribution shifts in both textual attributes and graph structure. Specifically, text attributes can vary widely, for example from scientific papers [14] to e-commerce product reviews [33]. Edge connection patterns can range from homophilic graphs such as citation networks, where papers on similar themes are linked [15], to heterophilic graphs such as webpages, which connect nodes with distinct topics [34]. Moreover, the labeling task itself can shift which requires a task-adaptive approach to process both textual features and network structure. Consequently, the core insight behind our model design is grounded in the following two key principles.

Principle I: Unifying the text space and obtaining task-adaptive embeddings. LLMs offer powerful text-understanding capabilities that naturally unify the textual feature space. However, to handle the large-scale graph aggregation discussed later, we require these capabilities to extend beyond raw text to an embedding space. Hence, we propose to adopt LLM-based encoder models such as LLM2Vec [35, 36] for text embedding. Although this approach might appear to be a naive extension of smaller LM-based embedding methods (e.g., those relying on SBERT [37] or RoBERTa [38]), we argue that leveraging the decoder-induced encoder structure of LLMs is essential for achieving task-adaptive embeddings. In particular, we introduce a novel prompting strategy that encodes text attributes conditioned on inference-task descriptions, enabling significantly improved zero-shot inference - an ability not readily achieved by smaller LM-based embeddings.

Principle II: Developing a generalizable adaptive graph information aggregation mechanism. Graph structure determines the node neighboring relationships and thus the information aggregation from which nodes may benefit the inference. Inspired by the belief propagation (BP) algorithm [39] that gives the optimal statistical inference over pairwise correlated random variables, we propose to regard the graph as a Markov Random Field (MRF), each node as a random variable, and mimic BP to aggregate information for node label inference. Because BP is rooted in basic mathematical principles, this approach is widely generalizable. Algorithmic adaptivity across different TAGs hinges on estimating the coupling coefficients in the graphs, which can be done by having LLMs analyze the attributes of sampled pairs of connected nodes. Moreover, this BP-inspired approach naturally adapts to varying levels of text attribute quality: nodes with higher-quality text attributes present greater influence on their neighbors, and vice versa.

By applying the two principles outlined above, we propose our new strategy, LLM-BP, for zero-shot inference over TAGs. LLM-BP does not require any training or fine-tuning. We evaluate LLM-BP on 11 real-world TAG datasets from various domains, including citation networks [14, 15, 40], e-commerce [33], knowledge graphs [34], and webpage networks [41], covering both homophilic and heterophilic graph structures.

Experimental results demonstrate the effectiveness of LLM-BP. Notably, our task-conditional embeddings (Principle I) improve performance by 8.10% on average compared to the best LM-based encoders. In addition, our BP-inspired aggregation mechanism (Principle II) provides an extra 1.71% performance gain with our embeddings, demonstrating strong generalization across both homophilic and heterophilic TAGs. Our experiments also reveal that current methods aligning graph-aggregated embeddings to LLM token spaces significantly underperform approaches that simply use smaller LM encoders without even incorporating graph structures. This outcome indicates that the primary source of

generalization in these methods is the smaller LM’s text embeddings, rather than LLM-based reasoning on embeddings. It reinforces our earlier argument that limited training data hinders effective alignment in this context, urging caution for future work considering this strategy.

2 Related Works

Here, we briefly review existing methods by examining how they enable model generalization across TAGs.

Tuning Smaller LM Encoders. These methods typically rely on a source-domain graph for training. Notable works include ZeroG [18] that tunes SBert [37] on source datasets to align class-description embeddings with node text, thereby enhancing zero-shot performance on target datasets. Another approach, UniGLM [19], fine-tunes BERT [42] using contrastive learning on source datasets to yield a more generalizable encoder. GNNs trained with UniGLM embeddings in a supervised manner outperform models that directly adopt LM embeddings.

Training GNNs for Generalization. These methods focus on leveraging graph structure in a generalizable manner. Among them, graph self-supervised learning [43] is particularly common for producing representations without labeled data, often employing contrastive learning or masked modeling [21, 20, 44]. GraphMOE is a more recent technique inspired by the success of mixture-of-experts [45], pre-training parallel graph experts targeting different structures or domains [46, 47, 48, 49]. Others also consider LM-GNN co-training including [50, 51] that also follow a contrastive learning idea. Note that, however, all these methods still require training.

In contrast to the above effort that adopts smaller LM encoders, works that involve the use of LLMs are reviewed in the following and may achieve better generalization. More related works including LLM-based data augmentations for GNN training for generalization and LLMs for other graph reasoning tasks can be found in Appendix. 6.

LLMs with Node-Text Input. LLMs being directly fed with raw node texts demonstrates strong zero-shot ability on TAGs [24, 52, 25]. However, they suffer from the limitation of not being able to incorporate graph structural information.

LLMs with Graph-Embedding Input. With smaller LM-encoded node embeddings, various strategies integrate graph structure by aggregating these embeddings, such as neighborhood-tree traversal or concatenating the averaged embeddings from different hops [26, 27, 28], or via pre-trained GNNs [30, 29]. As mentioned earlier, these methods rely on aligning embeddings with the LLMs’ token space. For instance, LLaGA [26] trains a simple MLP on citation networks and [29] employs a linear projector on the ogbn-Arxiv [53] dataset, both using the next-token prediction loss, while [27] adopts self-supervised structure-aware graph matching as the training objective. However, due to limited TAG-domain data, the space alignment in these methods often remains undertrained, leading to degraded performance.

Multi-Task Graph Foundation Models. More ambitious studies aim to generalize across various graph-related tasks within a single framework. Notable approaches include graph prompting [54], which introduces “prompting nodes” to transform diverse graph tasks into a unified format. These frameworks then train GNNs to address the tasks [18, 55, 47] or further integrate LLMs [56, 57]. Although these works are impressive, they still fail to achieve zero-shot performance comparable to those methods that focus on specific graph data domains.

3 Generalization Principles for LLM-BP

3.1 Notations and Problem Formulation

Let (\mathcal{G}, X, Y) represent a TAG of interest, where $\mathcal{G}(\mathcal{V}, \mathcal{E})$ denotes the graph structure, \mathcal{V} is the node set of size n , and \mathcal{E} is the edge set. The node textual attributes are represented as $X = \{X_1, \dots, X_n\}$, and each node belongs to one of c classes, with labels given by $Y = \{y_1, y_2, \dots, y_n\} \in [c]^n$.

The objective is to infer the labels of nodes in TAGs based on the node attributes and graph structure. This study primarily focuses on the **zero-shot** setting, where no labeled data are assumed to be available in advance. Additionally, a **few-shot** setting is considered, where k labeled nodes are known for each class. Due to space limitations, results for the few-shot setting are provided in Appendix 9.4.

3.2 Motivation and the Overall Framework

LLMs are commonly used as decoders for next-token prediction. While LLMs excel at processing natural language inputs, they are not inherently compatible with graph data. Recently, some studies have explored methods to integrate graph data into LLMs, primarily for reasoning tasks [58, 59, 60].

In the context of TAGs, accurate node label inference relies on effectively combining the attributes of multiple nodes, especially when a node’s individual attributes are insufficient to determine its label. However, as noted earlier, LLMs are constrained by limited context windows, making it challenging to process all attributes from the potentially large set of connected nodes. Traditional approaches to compressing graph structural information involve creating embeddings, such as using GNNs to aggregate information from the target node’s neighbors. While effective, these embedding methods do not seamlessly integrate with LLM inputs and often require non-trivial training effort to align the LLMs’ token space with the node embedding space [26, 29, 27].

Our approach, LLM-BP, does not confine LLMs to their traditional usage. We first leverage their capabilities to generate task-adaptive node embeddings. Then, instead of requiring LLMs to directly process these embeddings, LLMs are further employed to analyze graph data and provide generalizable guidance in aggregating these embeddings. These two steps are to match the two generalization principles proposed in Sec. 1. Classification is ultimately performed by computing the cosine similarity between the final node embeddings $\mathbf{h}^X = [h_1^X, \dots, h_n^X]$ and candidate class embeddings $\mathbf{q}^C = [q_1^C, \dots, q_c^C]$. In the zero-shot setting, class embeddings are generated as follows: we randomly sample $l \ll n$ nodes and employ LLMs to infer their labels. The embeddings of sampled nodes form distinct clusters based on LLMs’ prediction. We compute the average embedding of the embeddings closest to the cluster center to obtain the class embedding. In the few-shot setting, class embeddings are obtained by averaging the embeddings of labeled nodes within each class. See Appendix. 7.2 for details.

3.3 Principle I: Task-Adaptive Node Embeddings \mathbf{h}^X

Creating generalizable text embeddings is no longer a significant challenge. Even smaller LM encoders, such as SBert [37], are capable of achieving this. Indeed, most existing works utilize these encoders to generate initial node embeddings for TAGs [10, 26, 27, 29]. However, for these embeddings to be directly usable for label prediction without the need for additional transformation models, it is crucial to incorporate task-specific information. In other words, the embeddings must be tailored to the specific task, resulting in what we term task-adaptive embeddings.

Achieving task adaptivity, however, presents a notable challenge. Smaller LM encoders lack the expressive power necessary to encode nuanced task-specific information. This limitation motivates our adoption of LLM-induced encoders, driven by the emergent capabilities of LLMs in contextual learning [61, 62].

There have been recent advancements in extending LLMs to generate text embeddings [35, 63]. In our approach, we utilize a form of LLM2Vec [35], which transforms LLM decoders into encoders via retaining the unidirectional attention mechanism. Following the methodology in [36], we extract the output embedding of $\langle \text{response} \rangle$ - the token positioned immediately after the inputs - as the text embedding for the input node attributes.

To embed task-specific information into node embeddings, we propose a prompting strategy structured with the following template:

$$\langle \text{Instruct} \rangle \{ \text{task_description} \} \{ \text{class_info} \} \langle \text{query} \rangle X_i \langle \text{response} \rangle. \quad (1)$$

Here, $\langle \cdot \rangle$ encloses specific tokens. The task details are described in $\{ \text{task_description} \}$, and $\{ \text{class_info} \}$ contains the basic information of each class. An example is given in Fig. 1. The class information serves as a crucial contextual enhancement, enabling LLMs to generate embeddings in a conditioned manner. For more detailed on the class-conditional prompt for each dataset used in this study, refer to Appendix. 7.2 and 10.1.

3.4 Principle II: Generalizable Graph Aggregation

Graph structures can provide essential correlated information for node label inference by characterizing the relationships between node attributes and labels [64, 65, 66, 67, 68, 69]. Specifically, we may consider each node’s label and attributes as random variables, and each edge as a coupling between them for connected node pairs. The fundamental BP algorithm enables principled statistical inference over this set of correlated random variables [39]. Since BP is inherently agnostic to the application domain of the TAG, emulating BP offers a mechanism to aggregate correlation information encoded in the graph structure across domains.

Markov Random Field Modeling We consider the joint probability distribution $\mathbb{P}_{\mathcal{G}}(Y, X)$ over the graph where Y and X denotes the random variables of node labels and attributes, respectively. In $\mathbb{P}_{\mathcal{G}}(Y, X)$, the distribution over the node labels given the graph structure is denoted as

$$\mathbb{P}_{\mathcal{G}}(Y) = \frac{1}{Z_Y} \prod_{i \in \mathcal{V}} \phi_i(y_i) \prod_{(i,j) \in \mathcal{E}} \psi_{ij}(y_i, y_j). \quad (2)$$

Algorithm 1 LLM-BP

input TAG $(\mathcal{G}, \mathbf{X})$
output Class label prediction $\{\hat{y}_i\}_{i \in [n]}$

- 1: $\mathbf{h}^X \leftarrow$ Task-adaptive encoding following Eq. (1)
 - 2: **if** zero-shot **then**
 - 3: Sample $l \ll n$ nodes, infer labels with LLMs,
 - 4: Nodes clusters based on LLM prediction,
 - 5: $\mathbf{q}^C \leftarrow$ Average embedding of samples near center,
 - 6: **else if** few-shot **then**
 - 7: $\mathbf{q}^C \leftarrow$ Average embedding of k samples per class,
 - 8: **end if**
 - 9: Estimate $\psi_{ij}(y_i, y_j)$ by employing the LLM to analyze the graph data (e.g., using Eq. (6) based on the estimated homophily level r .)
 - 10: Initialize $p^{(0)}(y_i) \leftarrow$ Eq. (5) and $m_{i \rightarrow j}^{(0)}(y_j) = 1$
 - 11: Run LLM-BP (Eq. (4)) for L iterations or its approximation (Eq. (7)) for single iteration
 - 12: $\hat{y}_i \leftarrow \arg \max_{y_i} \log p_i^{(k)}(y_i; x_i)$
-

Here $\phi_i(y_i)$ denotes the unary potential for node i , $\psi_{ij}(y_i, y_j)$ is the edge potential capturing the correlation between labels y_i and y_j of adjacent nodes, and Z_Y is the normalization constant. For node attributes, MRF modeling assumes that each node's attributes are conditionally independent of others given the node labels, which can be characterized by the distribution:

$$\mathbb{P}_{\mathcal{G}}(X | Y) = \prod_{i \in \mathcal{V}} \mathbb{P}_{\mathcal{G}}(X_i | y_i) = \prod_{i \in \mathcal{V}} \varphi_{y_i}(X_i) \quad (3)$$

where $\varphi_{y_i}(X_i)$ captures the likelihood of having node i 's attributes X_i given its label y_i .

The proposed modeling approach is highly adaptive, as it can capture the varying graph connectivity patterns across different TAGs through interpretable edge potentials. For instance, $\psi_{ij}(y_i, y_j)$ represents the unnormalized likelihood that nodes with labels y_i and y_j are connected. This formulation naturally incorporates the modeling of graph homophily and heterophily: $\psi_{ij}(y_i, y_i) > \psi_{ij}(y_i, y_j)$ indicates homophily, while $\psi_{ij}(y_i, y_i) < \psi_{ij}(y_i, y_j)$ reflects heterophily. Furthermore, $\varphi_{y_i}(X_i)$ enables the model to account for variations in the quality of text attributes (w.r.t. their indicative power for the labels) across different TAGs, further enhancing its adaptivity. For node classification, we can infer $\mathbb{P}_{\mathcal{G}}(Y | X) \propto \prod_{i \in \mathcal{V}} \varphi_{X_i}(y_i) \prod_{(i,j) \in \mathcal{E}} \psi_{ij}(y_i, y_j)$ where $\varphi_{X_i}(y_i) = \varphi_{y_i}(X_i) \phi_i(y_i)$.

Belief Propagation Exact inference for $\mathbb{P}_{\mathcal{G}}(Y|X)$ is intractable in large-scale graphs with cycles [70]. In practice, loopy belief propagation (LBP) is often used to conduct an approximate inference [39], which follows: Initialize the distributions $p_j^{(0)}(y_j) \propto \varphi_{X_j}(y_j)$ and $m_{i \rightarrow j}^{(0)}(y_j) = 1/c$ for all $i, j \in \mathcal{V}$. For $k = 1, 2, \dots, L$, we do

$$\begin{aligned} \log m_{j \rightarrow i}^{(k)}(y_i) &\cong \text{LSE}_{y_j} [\log \psi_{ij}(y_i, y_j) + \\ &\quad \log p_j^{(k-1)}(y_j) - \log m_{i \rightarrow j}^{(k-1)}(y_j)], \\ \log p_i^{(k)}(y_i) &\cong \log p_i^{(0)}(y_i) + \sum_{j \in \mathcal{N}(i)} \log m_{j \rightarrow i}^{(k)}(y_i), \end{aligned} \quad (4)$$

where \cong denotes the equality with difference up-to a constant. LSE stands for the log-sum-exp function: $\text{LSE}_{y_j}[f(y_i, y_j)] = \log \left[\sum_{y_j} \exp(f(y_i, y_j)) \right]$. The final $\arg \max_{y_i} p_i^{(k)}(y_i)$ gives the label prediction. Detailed derivation can be found in Appendix. 8.

LLM-BP To execute the above LBP algorithm, we need to specify several components based on the TAG. First, $p_i^{(0)}(y_i)$ represents the distribution of the label y_i given the observed attributes X_i alone, which can be estimated using normalized cosine similarities:

$$p_i^{(0)}(y_i) = \text{softmax}(\{\cos(h_i^X, q_k^C)/\tau\}_{k \in [c]}) \quad (5)$$

where h_i^X and h_k^C denote node i 's class-conditional embedding and class k 's embedding given by the LLM encoder as discussed in the previous section. $\cos(\cdot)$ denotes cosine similarity and τ is the temperature hyper-parameter.

Second, we characterize the edge potentials $\psi_{ij}(y_i, y_j)$. We employ an LLM agent to assess the homophily level of the TAG. Specifically, we uniformly at random sample T connected node pairs ($T \ll |\mathcal{E}|$), and for each pair, we prompt the LLM to determine whether the two nodes belong to the same class based on their attributes, as illustrated in Fig. 1. The ratio of “Yes” responses, denoted by r is used to set

$$\psi_{ij}(y_i, y_j) = \begin{cases} r, & \text{if } y_i = y_j \\ 1 - r, & \text{if } y_i \neq y_j \end{cases}, \quad (6)$$

Note that a more complex $\psi_{ij}(y_i, y_j)$ can be adopted by estimating the edge probabilities between any two classes. However, we choose the homophily level as a proof of concept. LLMs can provide a reasonably accurate estimation of the homophily level, as pairwise comparisons are typically much simpler tasks compared to full-scale classification.

[69] demonstrated that linear propagation can approximate a single iteration of LBP when feature quality is limited. Based on this insight, we adopt the following approximate LBP formulation (denoted as BP appr.):

$$\log p_i^{(1)}(y_i) \cong \log p_i^{(0)}(y_i) + \text{sgn}\left(\log \frac{r}{1-r}\right) \sum_{j \in \mathcal{N}(i)} \log p_j^{(0)}(y_i), \quad (7)$$

where the homophily level r influences the sign of the log-likelihood aggregation from neighboring nodes. We summarize the overall pipeline in Algorithm. 1

4 Experiments

In this section, we evaluate LLM-BP based on its two design principles, with a primary focus on zero-shot node classification tasks. Evaluations of few-shot node classification and link prediction tasks are provided in Appendix. 9.4 9.5. First, we demonstrate the effectiveness of task-adaptive encoding and identify issues with existing methods that rely on aligning node embeddings with the LLM token space. Second, we validate the effectiveness of the proposed BP algorithm. Finally, we present the end-to-end performance of LLM-BP, comparing it to state-of-the-art baselines. We first introduce the datasets and baselines used in the study:

Datasets As listed in Table 1, we selected eleven real-world TAG datasets that encompass a variety of text domain shifts, including citation networks, e-commerce data, knowledge graphs, and webpage networks, which cover both homophily and heterophily structures. For more details, see Appendix 7.1.

Baselines: We select representative baselines from all existing categories for model generalization on TAGs:

- *Vanilla LM / LLM Encoders:* including SentenceBERT (SBert) [37], RoBERTa [38], text-embedding-3-large [71], and bge-en-icl [36], a state-of-the-art LLM2Vec encoder.
- *Vanilla LLMs:* including GPT-3.5-turbo [1] and GPT-4o [72], the latter being among the most advanced LLMs in reasoning. They process raw node texts without incorporating graph structures.
- *Tuning LM Encoder / GNNs:* including ZeroG [18], UniGLM [19] that tune LM encoders, ZeroG is specifically proposed for zero-shot node classification. DGI [21], GraphMAE [20] that perform Graph-SSL are also compared.
- *LLMs with Graph Adapters:* including LLaGA [26], TEA-GLM [29], and GraphGPT [27], which are the three representative works adopting LLMs with projectors to align compressed node representations with the token space.
- *Multi-Task Graph Foundation Models:* Consisting of OFA [55] and GOFA [57], which are the state-of-the-art multi-task foundation models.
- *LLMs for Data Augmentation:* referring to LLM-GNN [73], specifically designed for zero-shot node classification, which utilizes LLMs as annotators for pseudo-labels and further train GNNs for inference.
- *Neighborhood Aggregation (NA):* referring to the training-free method proposed in [56], which injects graph structural information into node representations by directly aggregating the averaged neighborhood embeddings.

Dataset	Text Domain	Graph Structure
Cora [14]	CS Publication	Homopholic
Citeseer [15]	CS Publication	Homopholic
Pubmed [40]	Medical Publication	Homopholic
History [33]	History Books	Homopholic
Children [33]	Children Literature	Homopholic
Sportsfit [33]	Sports Goods	Homopholic
Wikics [34]	Knowledge Graph	Homopholic
Cornell [41]	School Webpage	Heterophilic
Texas [41]	School Webpage	Heterophilic
Wisconsin [41]	School Webpage	Heterophilic
Washington [41]	School Webpage	Heterophilic

Table 1: TAG Datasets selected in experiments.

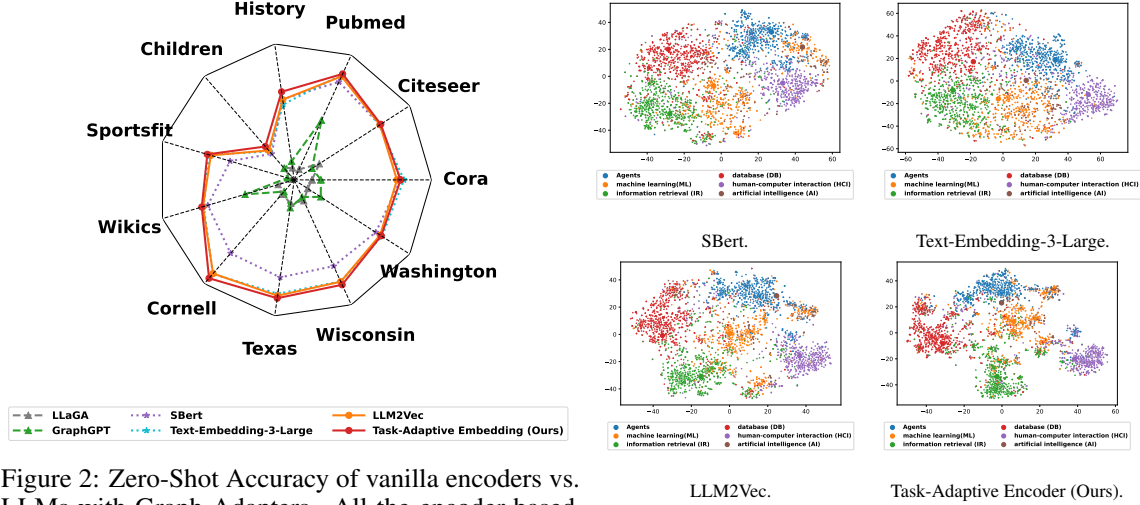


Figure 2: Zero-Shot Accuracy of vanilla encoders vs. LLMs-with-Graph-Adapters. All the encoder-based methods do not leverage graph structure information. Figure 3: t-SNE visualization of encoders on Citeseer.

Settings: Unlike LLM-BP which is training-free, most of the baselines—except from vanilla encoders, LLMs or NA—require pre-training. Methods of vanilla encoders and LLM-BP that require sampling nodes to obtain class embeddings under zero-shot settings are repeated 30 times with seed 42 to 71, and the average performance is reported in the following experiment sections. Implementation details for baselines and LLM-BP can be found in Appendix. 7.3 7.2.

4.1 Evaluation for Task-Adaptive Node Embedding

• **Exp.1: Ineffectiveness of LLMs w/ Graph Adapters** Figure 2 illustrates the accuracy of encoder-based methods alongside two representative LLMs-with-graph-adapters methods across each dataset. Notably, using text embeddings generated by SBert [37] without incorporating graph structural information significantly outperforms both LLaGA [26] and GraphGPT [27]. These two methods align node representations that combine SBert embeddings with graph information to the LLMs’ token space via a projector. This finding suggests that the generalization capabilities of these approaches primarily stem from the pre-trained language model encoders rather than the LLMs’ inherent understanding of TAG data. Consequently, future works should exercise caution when adopting this strategy.

• Exp.2: Effectiveness of The Task-Adaptive Encoder

According to Figure 2, the task-adaptive encoder achieves the best performance on most of the datasets, enhancing the vanilla LLM2Vec on average by 2.3%, highlighting the importance of incorporating task-specific information during encoding. To further illustrate this, we use the Citeseer [15] dataset as an example and perform t-SNE visualization [74] on the embeddings derived from the encoders. As shown in Fig. 3, when provided with class information, the task-adaptive encoder generates embeddings that exhibit tighter clustering for the same class compared to other baselines. The significance test of improvement from task-adaptive encoding is provided in Table. 5 in Appendix. 9.1.

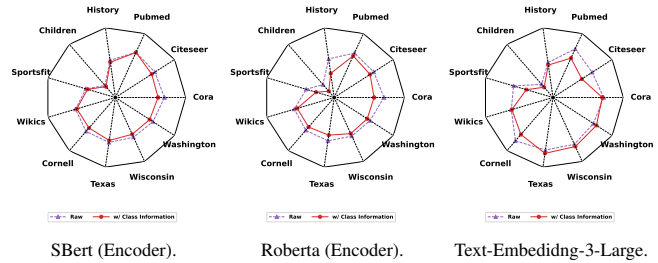


Figure 4: Class information fed into different encoders.

Note that the benefits of class information are observed only in encoders derived from LLM decoders potentially due to their strong contextual learning capabilities. As illustrated in Fig. 4, incorporating class information into smaller LM encoders, such as SBert [37] or RoBERTa [38], may even degrade performance. Regarding Text-embedding-3-large [71], the impact of class information remains inconclusive due to the unknown internal mechanisms of the black-box encoder.

4.2 Generalizable Graph Aggregation

	Homophilic														Heterophilic										Avg Rank	
Method	Citation Graph						E-Commerce & Knowledge Graph								Schools						Acc		F1			
	Cora		Citeseer		Pubmed		History		Children		Sportsfit		Wikics		Cornell		Texas		Wisconsin						Washington	
	Acc	F1	Acc	F1	Acc	F1	Acc	F1	Acc	F1	Acc	F1	Acc	F1	Acc	F1	Acc	F1	Acc	F1	Acc	F1	Acc	F1		
Text-Embedding-3-Large [71]	Sbert [37]	69.75	67.21	66.69	63.31	70.57	71.38	53.53	20.45	22.59	20.13	43.79	38.26	59.06	56.19	63.66	54.39	64.58	49.79	62.10	52.07	63.52	48.00	7.27	7.09	
	Roberta [38]	70.71	68.47	66.95	63.57	69.54	70.31	55.39	21.84	24.25	22.41	41.51	36.09	59.08	56.49	61.68	51.84	62.25	49.26	60.33	49.08	60.60	45.34	7.18	7.18	
	LLM2Vec [35]	71.90	69.87	66.24	63.30	75.96	75.75	50.15	19.21	24.68	24.10	58.39	53.03	61.78	58.82	81.50	70.11	75.42	63.17	73.14	63.02	66.35	57.69	5.36	4.45	
	SBert + NA [56]	67.34	65.92	67.13	64.37	74.57	74.65	53.14	19.06	25.56	24.31	57.00	52.29	62.34	58.32	81.26	69.08	76.68	63.12	73.36	62.50	65.92	53.34	5.64	5.36	
	GPT-3.5-turbo [1]	72.49	69.90	68.66	64.75	71.26	71.87	57.86	21.98	25.28	22.74	46.84	40.85	66.26	63.57	54.21	44.66	56.04	41.09	54.23	46.11	58.88	43.05	5.82	6.00	
GPT-4o [72]	GPT-3.5-turbo [1]	70.11	52.11	66.83	47.58	89.75	66.16	55.07	30.36	29.73	26.13	67.21	54.45	65.53	51.19	45.54	39.30	56.14	32.53	58.86	46.84	51.09	35.68	5.64	8.18	
	GPT-4o [72]	70.29	62.95	64.77	47.78	89.85	67.39	53.30	31.68	30.76	29.20	66.35	56.22	66.10	56.04	45.54	41.92	63.10	50.51	56.60	52.54	48.90	42.54	5.91	6.36	
UniGLM [19]	ZeroG [18]	45.57	43.25	52.26	48.41	70.33	69.78	44.24	24.84	21.48	19.17	33.46	32.99	55.05	52.08	23.03	22.06	21.39	18.90	27.16	26.45	24.01	23.08	11.36	9.91	
	DGI [21]	60.4	56.02	50.35	45.15	74.68	71.75	36.55	16.84	12.72	12.61	14.27	5.33	46.74	40.86	10.47	6.46	53.48	15.95	12.66	5.02	8.3	3.07	12.27	12.73	
GraphMAE [20]	OFA [55]	16.79	12.77	15.24	15.04	25.10	19.18	20.98	3.89	2.22	1.04	7.48	3.47	14.98	4.24	14.66	10.02	11.23	9.42	12.08	6.95	20.96	14.15	13.91	14.73	
	GOFa [57]	15.13	7.10	8.11	7.67	36.56	34.29	36.36	5.75	7.24	1.97	30.50	6.99	8.91	4.03	23.04	14.95	17.65	11.67	23.02	11.87	24.89	13.34	15.18	15.45	
GraphGPT [27]	LLaGA [26]	20.36	16.57	41.31	33.37	28.18	26.62	8.25	3.48	3.05	2.29	15.18	4.7	30.77	25.22	29.84	12.62	11.77	5.87	4.8	3.44	6.04	4.28	13.91	14.73	
	LLM-BP	71.06	70.21	65.72	64.18	74.76	73.00	56.25	31.57	12.15	7.73	37.87	33.19	68.62	62.93	39.50	35.47	38.37	29.54	32.51	25.12	31.02	21.24	8.00	7.45	
LLM-BP (appr.)	LLM-BP	17.48	12.68	13.93	12.78	42.94	25.68	12.31	9.15	9.94	4.24	4.53	2.44	33.59	30.21	10.18	14.71	18.48	9.85	12.35	6.32	20.64	15.79	14.55	14.64	
	LLM-BP (appr.)	11.62	14.42	19.52	23.34	7.56	13.42	7.95	8.89	10.09	5.02	1.84	2.66	10.98	16.73	12.57	20.1	15.51	22.97	15.09	20.85	10.48	18.98	15.36	13.64	
	LLM-BP	72.59	71.10	69.51	66.29	75.55	75.32	59.86	22.66	24.81	22.66	61.92	57.51	67.75	63.53	83.28	71.80	81.66	65.41	77.75	63.70	73.14	57.33	2.27	2.55	
	LLM-BP (appr.)	71.41	70.11	68.66	65.62	76.81	76.81	59.49	23.02	29.40	28.45	61.51	57.09	67.96	64.27	84.92	74.19	79.39	64.63	75.65	62.53	70.04	55.53	2.45	2.27	

Table 2: Zero-Shot End-to-End Evaluation. ‘NA’ refers to neighborhood embedding aggregation.

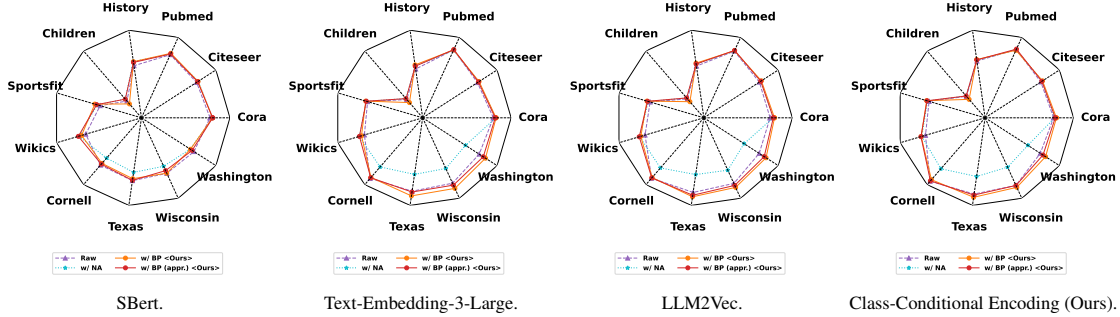
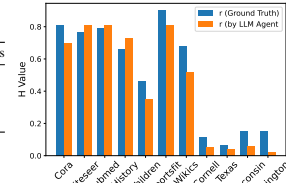


Figure 6: Experiments on graph information aggregation. ‘Raw’ refers no graph structure usage, ‘w/ NA’ refers to the neighborhood embedding aggregation (NA) proposed in [56], ‘w/ BP’ refers to the belief propagation following Eq. 6, ‘w/ BP (appr.)’ refers to its simplified linear form that follows Eq. 7.

• Exp.3: LLM Agents for Homophily Level r Estimation

As shown in Fig.5 (Left), we randomly sample k edges ($k = 100$ for large graphs and $k = 50$ for small ones), incorporating them into prompts (Fig.1) for LLM-based estimation of the homophily level r (Sec.3.4). We evaluate four LLMs: GPT-4o, GPT-4o-mini[72], GPT-3.5-Turbo [1], and Mistral-7B-Instruct v0.3 [75]. Each model responds to each node pair over five trials, with the final estimate determined by majority voting. Full results are provided in Fig.7 in appendix, demonstrating that GPT-4o-mini and GPT-4o effectively estimate r , GPT-3.5-Turbo performs reasonably well, while Mistral-7B-Instruct-v0.3 fails. Balancing accuracy and cost efficiency, we select GPT-4o-mini’s estimation (Fig. 5 Right) for subsequent studies.

Graph Type	# Sampled Edges
Citation	100
E-Commerce	100
Knowledge Graph	100
Web Page	50


 Figure 5: Left: Number of edges sampled per dataset. Right: GPT-4o-mini’s prediction of the homophily level r .

• Exp.4: Effectiveness of the BP Algorithm

Experimental results are presented in Fig. 6, where we evaluate the four approaches over various graph structures. Specifically, We compare the BP algorithm (Eq. 6) and its linear approximation (Eq. 7) with vanilla encoders that do not utilize structure (Raw) and the NA baseline. For all the four encoders across all the datasets, the proposed BP algorithm slightly outperforms its linear approximation, and they consistently outperform Raw. Moreover, in most datasets, they also surpass the NA baseline, particularly on heterophilic graphs, where direct neighborhood embedding aggregation negatively affects performance. These results highlight the generalizability of our data modeling approach and the effectiveness of the key-parameter estimation design in BP.

4.3 End-to-End Evaluation

• Exp.5: Main Results in the Zero-Shot Setting

The main experimental results are presented in Table 2. Among the baselines, vanilla encoders and LLMs demonstrate strong zero-shot generalization. GPT-3.5-Turbo [1] ranks first on the Sportsfit dataset, while GPT-4o [72] achieves the best performance on Pubmed and Children.

UniGLM [19] and ZeroG [18] perform well in domains aligned with their pre-training, such as citation networks (e.g., ZeroG enhances SBert’s performance on Cora, Pubmed, and Wikics). However, both struggle on TAGs with unseen

text distributions (e.g., Sportsfit) or novel graph structures (e.g., webpage networks), suggesting that fine-tuned LM encoders may suffer performance degradation on out-of-domain TAGs. Similarly, graph-SSL methods (DGI [21], GraphMAE [20]) show limited generalization across structural shifts.

Among multi-task graph foundation models, GOFA achieves strong performance, likely benefiting from a larger pre-training corpus for graph-text alignment [76, 77] compared to GraphGPT [27] and LLaGA [26], which are trained solely on ogbn-arxiv. However, GOFA still requires broader pre-training and instruction fine-tuning to improve generalization under text domain shifts, and its reliance on GNNs may limit effectiveness on heterophilic data.

Notably, LLM-BP and LLM-BP (appr.) achieve the highest average ranking across all datasets. Another interesting observation is that when we randomly sample 20c nodes to obtain the class embeddings with the help of LLMs following Algorithm. 1, the zero-shot performance of the encoders in this setting is comparable to their performance between 5-10-shot setting as shown in Table. 8 in the Appendix. Further comparisons with LLM-GNN [73] and TEA-GLM [29] are provided in Appendix 9.3.

• **Exp.6: Main Results under Few-shot Setting** We conduct the evaluation in $k = 1, 3, 5, 10$ -shot settings. Using 10 different random seeds, we sample the shots from the training set and repeat the experiments 10 times. The experimental results are presented in Table 8 in Appendix 9. Across all k -shot settings, LLM-BP and LLM-BP (appr.) outperform the baseline models.

5 Discussion and Limitations

Graph learning tasks often face substantial data constraints compared to other domains, underscoring the importance of establishing fundamental principles that foster model generalization. Our approach exemplifies this by leveraging LLMs to analyze graph data and determine suitable inference strategies, particularly via homophily estimation for belief propagation. While LLM-BP achieves notable success on TAGs for node classification and extends partially to link prediction, it remains a step away from a fully comprehensive graph foundation model that addresses a wider range of graph learning tasks. Nonetheless, the core idea of leveraging LLM-driven graph analysis to guide algorithmic decisions aligned with task-specific inductive biases holds broad potential for future applications.

Acknowledgments

H. Wang, S. Liu, R. Wei and Dr. P. Li are partially supported by NSF awards IIS-2239565, CCF-2402816, IIS-2428777, PHY-2117997; DOE award DE-FOA-0002785; JPMC faculty awards; Microsoft Azure Research Credits for Generative AI; and Meta research award.

We extend our sincere gratitude to Dr. Hongbin Pei, Dr. Zhen Wang, and Jingcheng Cen for their valuable assistance in identifying the raw node text of the heterophilic graphs used in this study.

References

- [1] Josh Achiam, Steven Adler, Sandhini Agarwal, Lama Ahmad, Ilge Akkaya, Florencia Leoni Aleman, Diogo Almeida, Janko Altenschmidt, Sam Altman, Shyamal Anadkat, et al. Gpt-4 technical report. *arXiv preprint arXiv:2303.08774*, 2023.
- [2] Ze Liu, Yutong Lin, Yue Cao, Han Hu, Yixuan Wei, Zheng Zhang, Stephen Lin, and Baining Guo. Swin transformer: Hierarchical vision transformer using shifted windows. In *Proceedings of the IEEE/CVF international conference on computer vision*, pages 10012–10022, 2021.
- [3] Alec Radford, Jong Wook Kim, Chris Hallacy, Aditya Ramesh, Gabriel Goh, Sandhini Agarwal, Girish Sastry, Amanda Askell, Pamela Mishkin, Jack Clark, et al. Learning transferable visual models from natural language supervision. In *International conference on machine learning*, pages 8748–8763. PMLR, 2021.
- [4] Jiawei Liu, Cheng Yang, Zhiyuan Lu, Junze Chen, Yibo Li, Mengmei Zhang, Ting Bai, Yuan Fang, Lichao Sun, Philip S Yu, et al. Towards graph foundation models: A survey and beyond. *arXiv preprint arXiv:2310.11829*, 2023.
- [5] Haitao Mao, Zhikai Chen, Wenzhuo Tang, Jianan Zhao, Yao Ma, Tong Zhao, Neil Shah, Michael Galkin, and Jiliang Tang. Graph foundation models. *arXiv preprint arXiv:2402.02216*, 2024.
- [6] Haiteng Zhao, Shengchao Liu, Ma Chang, Hannan Xu, Jie Fu, Zhihong Deng, Lingpeng Kong, and Qi Liu. Gimlet: A unified graph-text model for instruction-based molecule zero-shot learning. *Advances in Neural Information Processing Systems*, 36:5850–5887, 2023.

- [7] Wenqi Fan, Shijie Wang, Jiani Huang, Zhikai Chen, Yu Song, Wenzhuo Tang, Haitao Mao, Hui Liu, Xiaorui Liu, Dawei Yin, et al. Graph machine learning in the era of large language models (llms). *arXiv preprint arXiv:2404.14928*, 2024.
- [8] Xiaoxin He, Xavier Bresson, Thomas Laurent, Adam Perold, Yann LeCun, and Bryan Hooi. Harnessing explanations: Llm-to-lm interpreter for enhanced text-attributed graph representation learning. *ICLR*, 2024.
- [9] Yuhan Li, Peisong Wang, Xiao Zhu, Aochuan Chen, Haiyun Jiang, Deng Cai, Victor Wai Kin Chan, and Jia Li. Glbenc: A comprehensive benchmark for graph with large language models. *arXiv preprint arXiv:2407.07457*, 2024.
- [10] Zhikai Chen, Haitao Mao, Jingzhe Liu, Yu Song, Bingheng Li, Wei Jin, Bahare Fatemi, Anton Tsitsulin, Bryan Perozzi, Hui Liu, et al. Text-space graph foundation models: Comprehensive benchmarks and new insights. *arXiv preprint arXiv:2406.10727*, 2024.
- [11] Jiarui Feng, Hao Liu, Lecheng Kong, Mingfang Zhu, Yixin Chen, and Muhan Zhang. Taglas: An atlas of text-attributed graph datasets in the era of large graph and language models. *arXiv preprint arXiv:2406.14683*, 2024.
- [12] Zhuofeng Li, Zixing Gou, Xiangnan Zhang, Zhongyuan Liu, Sirui Li, Yuntong Hu, Chen Ling, Zheng Zhang, and Liang Zhao. Teg-db: A comprehensive dataset and benchmark of textual-edge graphs. *arXiv preprint arXiv:2406.10310*, 2024.
- [13] Jesús Bobadilla, Fernando Ortega, Antonio Hernando, and Abraham Gutiérrez. Recommender systems survey. *Knowledge-based systems*, 46:109–132, 2013.
- [14] Andrew Kachites McCallum, Kamal Nigam, Jason Rennie, and Kristie Seymore. Automating the construction of internet portals with machine learning. *Information Retrieval*, 3:127–163, 2000.
- [15] C Lee Giles, Kurt D Bollacker, and Steve Lawrence. Citeseer: An automatic citation indexing system. In *Proceedings of the third ACM conference on Digital libraries*, pages 89–98, 1998.
- [16] Srijan Kumar, Francesca Spezzano, VS Subrahmanian, and Christos Faloutsos. Edge weight prediction in weighted signed networks. In *Data Mining (ICDM), 2016 IEEE 16th International Conference on*, pages 221–230. IEEE, 2016.
- [17] Srijan Kumar, Bryan Hooi, Disha Makhija, Mohit Kumar, Christos Faloutsos, and VS Subrahmanian. Rev2: Fraudulent user prediction in rating platforms. In *Proceedings of the Eleventh ACM International Conference on Web Search and Data Mining*, pages 333–341. ACM, 2018.
- [18] Yuhan Li, Peisong Wang, Zhixun Li, Jeffrey Xu Yu, and Jia Li. Zerog: Investigating cross-dataset zero-shot transferability in graphs. In *Proceedings of the 30th ACM SIGKDD Conference on Knowledge Discovery and Data Mining*, pages 1725–1735, 2024.
- [19] Yi Fang, Dongzhe Fan, Sirui Ding, Ninghao Liu, and Qiaoyu Tan. Uniglm: Training one unified language model for text-attributed graphs. *arXiv preprint arXiv:2406.12052*, 2024.
- [20] Zhenyu Hou, Xiao Liu, Yukuo Cen, Yuxiao Dong, Hongxia Yang, Chunjie Wang, and Jie Tang. Graphmae: Self-supervised masked graph autoencoders. In *Proceedings of the 28th ACM SIGKDD Conference on Knowledge Discovery and Data Mining*, pages 594–604, 2022.
- [21] Petar Veličković, William Fedus, William L Hamilton, Pietro Liò, Yoshua Bengio, and R Devon Hjelm. Deep graph infomax. *arXiv preprint arXiv:1809.10341*, 2018.
- [22] Jared Kaplan, Sam McCandlish, Tom Henighan, Tom B Brown, Benjamin Chess, Rewon Child, Scott Gray, Alec Radford, Jeffrey Wu, and Dario Amodei. Scaling laws for neural language models. *arXiv preprint arXiv:2001.08361*, 2020.
- [23] Jie Huang and Kevin Chen-Chuan Chang. Towards reasoning in large language models: A survey. *arXiv preprint arXiv:2212.10403*, 2022.
- [24] Zhikai Chen, Haitao Mao, Hang Li, Wei Jin, Hongzhi Wen, Xiaochi Wei, Shuaiqiang Wang, Dawei Yin, Wenqi Fan, Hui Liu, et al. Exploring the potential of large language models (llms) in learning on graphs. *ACM SIGKDD Explorations Newsletter*, 25(2):42–61, 2024.
- [25] Rui Li, Jiwei Li, Jiawei Han, and Guoyin Wang. Similarity-based neighbor selection for graph llms. *arXiv preprint arXiv:2402.03720*, 2024.
- [26] Runjin Chen, Tong Zhao, Ajay Jaiswal, Neil Shah, and Zhangyang Wang. Llaga: Large language and graph assistant. *arXiv preprint arXiv:2402.08170*, 2024.

- [27] Jiabin Tang, Yuhao Yang, Wei Wei, Lei Shi, Lixin Su, Suqi Cheng, Dawei Yin, and Chao Huang. Graphgpt: Graph instruction tuning for large language models. In *Proceedings of the 47th International ACM SIGIR Conference on Research and Development in Information Retrieval*, pages 491–500, 2024.
- [28] Haitong Luo, Xuying Meng, Suhang Wang, Tianxiang Zhao, Fali Wang, Hanyun Cao, and Yujun Zhang. Enhance graph alignment for large language models. *arXiv preprint arXiv:2410.11370*, 2024.
- [29] Duo Wang, Yuan Zuo, Fengzhi Li, and Junjie Wu. Llm as zero-shot graph learners: Alignment of gnn representations with llm token embeddings. *arXiv preprint arXiv:2408.14512*, 2024.
- [30] Mengmei Zhang, Mingwei Sun, Peng Wang, Shen Fan, Yanhu Mo, Xiaoxiao Xu, Hong Liu, Cheng Yang, and Chuan Shi. Graphtranslator: Aligning graph model to large language model for open-ended tasks. In *Proceedings of the ACM on Web Conference 2024*, pages 1003–1014, 2024.
- [31] Xiaohua Zhai, Basil Mustafa, Alexander Kolesnikov, and Lucas Beyer. Sigmoid loss for language image pre-training. In *Proceedings of the IEEE/CVF International Conference on Computer Vision*, pages 11975–11986, 2023.
- [32] Christoph Schuhmann, Romain Beaumont, Richard Vencu, Cade Gordon, Ross Wightman, Mehdi Cherti, Theo Coombes, Aarush Katta, Clayton Mullis, Mitchell Wortsman, et al. Laion-5b: An open large-scale dataset for training next generation image-text models. *Advances in Neural Information Processing Systems*, 35:25278–25294, 2022.
- [33] Jianmo Ni, Jiacheng Li, and Julian McAuley. Justifying recommendations using distantly-labeled reviews and fine-grained aspects. In *Proceedings of the 2019 conference on empirical methods in natural language processing and the 9th international joint conference on natural language processing (EMNLP-IJCNLP)*, pages 188–197, 2019.
- [34] Péter Mernyei and Cătălina Cangea. Wiki-cs: A wikipedia-based benchmark for graph neural networks. *arXiv preprint arXiv:2007.02901*, 2020.
- [35] Parishad BehnamGhader, Vaibhav Adlakha, Marius Mosbach, Dzmitry Bahdanau, Nicolas Chapados, and Siva Reddy. Llm2vec: Large language models are secretly powerful text encoders. *arXiv preprint arXiv:2404.05961*, 2024.
- [36] Chaofan Li, MingHao Qin, Shitao Xiao, Jianlyu Chen, Kun Luo, Yingxia Shao, Defu Lian, and Zheng Liu. Making text embedders few-shot learners. *arXiv preprint arXiv:2409.15700*, 2024.
- [37] N Reimers. Sentence-bert: Sentence embeddings using siamese bert-networks. *arXiv preprint arXiv:1908.10084*, 2019.
- [38] Yinhan Liu. Roberta: A robustly optimized bert pretraining approach. *arXiv preprint arXiv:1907.11692*, 364, 2019.
- [39] Kevin Murphy, Yair Weiss, and Michael I Jordan. Loopy belief propagation for approximate inference: An empirical study. *arXiv preprint arXiv:1301.6725*, 2013.
- [40] Prithviraj Sen, Galileo Namata, Mustafa Bilgic, Lise Getoor, Brian Galligher, and Tina Eliassi-Rad. Collective classification in network data. *AI magazine*, 29(3):93–93, 2008.
- [41] Mark Craven, Dan DiPasquo, Dayne Freitag, Andrew McCallum, Tom Mitchell, Kamal Nigam, and Seán Slattery. Learning to extract symbolic knowledge from the world wide web. *AAAI/IAAI*, 3(3.6):2, 1998.
- [42] Jacob Devlin Ming-Wei Chang Kenton and Lee Kristina Toutanova. Bert: Pre-training of deep bidirectional transformers for language understanding. In *Proceedings of naacl-HLT*, volume 1. Minneapolis, Minnesota, 2019.
- [43] Yixin Liu, Ming Jin, Shirui Pan, Chuan Zhou, Yu Zheng, Feng Xia, and S Yu Philip. Graph self-supervised learning: A survey. *IEEE transactions on knowledge and data engineering*, 35(6):5879–5900, 2022.
- [44] Haihong Zhao, Aochuan Chen, Xiangguo Sun, Hong Cheng, and Jia Li. All in one and one for all: A simple yet effective method towards cross-domain graph pretraining. In *Proceedings of the 30th ACM SIGKDD Conference on Knowledge Discovery and Data Mining*, pages 4443–4454, 2024.
- [45] Noam Shazeer, Azalia Mirhoseini, Krzysztof Maziarz, Andy Davis, Quoc Le, Geoffrey Hinton, and Jeff Dean. Outrageously large neural networks: The sparsely-gated mixture-of-experts layer. *arXiv preprint arXiv:1701.06538*, 2017.
- [46] Zhenyu Hou, Haozhan Li, Yukuo Cen, Jie Tang, and Yuxiao Dong. Graphalign: Pretraining one graph neural network on multiple graphs via feature alignment. *arXiv preprint arXiv:2406.02953*, 2024.

- [47] Jingzhe Liu, Haitao Mao, Zhikai Chen, Wenqi Fan, Mingxuan Ju, Tong Zhao, Neil Shah, and Jiliang Tang. One model for one graph: A new perspective for pretraining with cross-domain graphs. *arXiv preprint arXiv:2412.00315*, 2024.
- [48] Lianghao Xia and Chao Huang. Anygraph: Graph foundation model in the wild. 2024.
- [49] Yijian Qin, Xin Wang, Ziwei Zhang, and Wenwu Zhu. Disentangled representation learning with large language models for text-attributed graphs. *arXiv preprint arXiv:2310.18152*, 2023.
- [50] Yufei He and Bryan Hooi. Unigraph: Learning a cross-domain graph foundation model from natural language. *arXiv preprint arXiv:2402.13630*, 2024.
- [51] Yun Zhu, Haizhou Shi, Xiaotang Wang, Yongchao Liu, Yaoke Wang, Boci Peng, Chuntao Hong, and Siliang Tang. Graphclip: Enhancing transferability in graph foundation models for text-attributed graphs. *arXiv preprint arXiv:2410.10329*, 2024.
- [52] Xuanwen Huang, Kaiqiao Han, Yang Yang, Dezheng Bao, Quanjin Tao, Ziwei Chai, and Qi Zhu. Can gnn be good adapter for llms? In *Proceedings of the ACM on Web Conference 2024*, pages 893–904, 2024.
- [53] Weihua Hu, Matthias Fey, Marinka Zitnik, Yuxiao Dong, Hongyu Ren, Bowen Liu, Michele Catasta, and Jure Leskovec. Open graph benchmark: Datasets for machine learning on graphs. *Advances in neural information processing systems*, 33:22118–22133, 2020.
- [54] Zemin Liu, Xingtong Yu, Yuan Fang, and Xinming Zhang. Graphprompt: Unifying pre-training and downstream tasks for graph neural networks. In *Proceedings of the ACM Web Conference 2023*, pages 417–428, 2023.
- [55] Hao Liu, Jiarui Feng, Lecheng Kong, Ningyue Liang, Dacheng Tao, Yixin Chen, and Muhan Zhang. One for all: Towards training one graph model for all classification tasks. *arXiv preprint arXiv:2310.00149*, 2023.
- [56] Haotong Yang, Xiyuan Wang, Qian Tao, Shuxian Hu, Zhouchen Lin, and Muhan Zhang. Gf-fusion: Rethinking the combination of graph neural network and large language model. *arXiv preprint arXiv:2412.06849*, 2024.
- [57] Lecheng Kong, Jiarui Feng, Hao Liu, Chengsong Huang, Jiaxin Huang, Yixin Chen, and Muhan Zhang. Gofa: A generative one-for-all model for joint graph language modeling. *arXiv preprint arXiv:2407.09709*, 2024.
- [58] Bryan Perozzi, Bahare Fatemi, Dustin Zelle, Anton Tsitsulin, Mehran Kazemi, Rami Al-Rfou, and Jonathan Halcrow. Let your graph do the talking: Encoding structured data for llms. *arXiv preprint arXiv:2402.05862*, 2024.
- [59] Yizhuo Zhang, Heng Wang, Shangbin Feng, Zhaoxuan Tan, Xiaochuang Han, Tianxing He, and Yulia Tsvetkov. Can llm graph reasoning generalize beyond pattern memorization? *arXiv preprint arXiv:2406.15992*, 2024.
- [60] Jianheng Tang, Qifan Zhang, Yuhao Li, and Jia Li. Grapharena: Benchmarking large language models on graph computational problems. *arXiv preprint arXiv:2407.00379*, 2024.
- [61] Pranab Sahoo, Ayush Kumar Singh, Sriparna Saha, Vinija Jain, Samrat Mondal, and Aman Chadha. A systematic survey of prompt engineering in large language models: Techniques and applications. *arXiv preprint arXiv:2402.07927*, 2024.
- [62] Banghao Chen, Zhaofeng Zhang, Nicolas Langrené, and Shengxin Zhu. Unleashing the potential of prompt engineering in large language models: a comprehensive review. *arXiv preprint arXiv:2310.14735*, 2023.
- [63] Niklas Muennighoff, Nouamane Tazi, Loïc Magne, and Nils Reimers. Mteb: Massive text embedding benchmark. *arXiv preprint arXiv:2210.07316*, 2022.
- [64] Xiaojin Zhu, Zoubin Ghahramani, and John D Lafferty. Semi-supervised learning using gaussian fields and harmonic functions. In *Proceedings of the 20th International conference on Machine learning (ICML-03)*, pages 912–919, 2003.
- [65] Thomas N Kipf and Max Welling. Semi-supervised classification with graph convolutional networks. *arXiv preprint arXiv:1609.02907*, 2016.
- [66] Petar Veličković, Guillem Cucurull, Arantxa Casanova, Adriana Romero, Pietro Lio, and Yoshua Bengio. Graph attention networks. *arXiv preprint arXiv:1710.10903*, 2017.
- [67] Will Hamilton, Zitao Ying, and Jure Leskovec. Inductive representation learning on large graphs. *Advances in neural information processing systems*, 30, 2017.
- [68] Jiong Zhu, Yujun Yan, Lingxiao Zhao, Mark Heimann, Leman Akoglu, and Danai Koutra. Beyond homophily in graph neural networks: Current limitations and effective designs. *Advances in neural information processing systems*, 33:7793–7804, 2020.

- [69] Rongzhe Wei, Haoteng Yin, Junteng Jia, Austin R Benson, and Pan Li. Understanding non-linearity in graph neural networks from the bayesian-inference perspective. *Advances in Neural Information Processing Systems*, 35:34024–34038, 2022.
- [70] Daphane Koller. Probabilistic graphical models: Principles and techniques, 2009.
- [71] OpenAI. Gpt text-embedding-3-large, 2024.
- [72] Aaron Hurst, Adam Lerer, Adam P Goucher, Adam Perelman, Aditya Ramesh, Aidan Clark, AJ Ostrow, Akila Welihinda, Alan Hayes, Alec Radford, et al. Gpt-4o system card. *arXiv preprint arXiv:2410.21276*, 2024.
- [73] Zhikai Chen, Haitao Mao, Hongzhi Wen, Haoyu Han, Wei Jin, Haiyang Zhang, Hui Liu, and Jiliang Tang. Label-free node classification on graphs with large language models (llms). *ICLR*, 2024.
- [74] Laurens Van der Maaten and Geoffrey Hinton. Visualizing data using t-sne. *Journal of machine learning research*, 9(11), 2008.
- [75] Albert Q Jiang, Alexandre Sablayrolles, Arthur Mensch, Chris Bamford, Devendra Singh Chaplot, Diego de las Casas, Florian Bressand, Gianna Lengyel, Guillaume Lample, Lucile Saulnier, et al. Mistral 7b. *arXiv preprint arXiv:2310.06825*, 2023.
- [76] Weihua Hu, Matthias Fey, Hongyu Ren, Maho Nakata, Yuxiao Dong, and Jure Leskovec. Ogb-lsc: A large-scale challenge for machine learning on graphs. *arXiv preprint arXiv:2103.09430*, 2021.
- [77] Ning Ding, Yulin Chen, Bokai Xu, Yujia Qin, Zhi Zheng, Shengding Hu, Zhiyuan Liu, Maosong Sun, and Bowen Zhou. Enhancing chat language models by scaling high-quality instructional conversations. *arXiv preprint arXiv:2305.14233*, 2023.
- [78] Taiyan Zhang, Renchi Yang, Mingyu Yan, Xiaochun Ye, Dongrui Fan, and Yurui Lai. Cost-effective label-free node classification with llms. *arXiv preprint arXiv:2412.11983*, 2024.
- [79] Lijie Hu, Huanyi Xie, Lu Yu, Tianhao Huang, Longfei Li, Meng Li, JUN ZHOU, and Di Wang. Low-cost enhancer for text attributed graph learning via graph alignment. 2024.
- [80] Bo Pan, Zheng Zhang, Yifei Zhang, Yuntong Hu, and Liang Zhao. Distilling large language models for text-attributed graph learning. In *Proceedings of the 33rd ACM International Conference on Information and Knowledge Management*, pages 1836–1845, 2024.
- [81] Jianxiang Yu, Yuxiang Ren, Chenghua Gong, Jiaqi Tan, Xiang Li, and Xuechang Zhang. Empower text-attributed graphs learning with large language models (llms). *arXiv preprint arXiv:2310.09872*, 2023.
- [82] Quan Li, Tianxiang Zhao, Lingwei Chen, Junjie Xu, and Suhang Wang. Enhancing graph neural networks with limited labeled data by actively distilling knowledge from large language models. *arXiv preprint arXiv:2407.13989*, 2024.
- [83] Xinnan Dai, Haohao Qu, Yifen Shen, Bohang Zhang, Qihao Wen, Wenqi Fan, Dongsheng Li, Jiliang Tang, and Caihua Shan. How do large language models understand graph patterns? a benchmark for graph pattern comprehension. *arXiv preprint arXiv:2410.05298*, 2024.
- [84] Zike Yuan, Ming Liu, Hui Wang, and Bing Qin. Gracore: Benchmarking graph comprehension and complex reasoning in large language models. *arXiv preprint arXiv:2407.02936*, 2024.
- [85] Sheng Ouyang, Yulan Hu, Ge Chen, and Yong Liu. Gundam: Aligning large language models with graph understanding. *arXiv preprint arXiv:2409.20053*, 2024.
- [86] Nuo Chen, Yuhan Li, Jianheng Tang, and Jia Li. Graphwiz: An instruction-following language model for graph computational problems. In *Proceedings of the 30th ACM SIGKDD Conference on Knowledge Discovery and Data Mining*, pages 353–364, 2024.
- [87] Yukun Cao, Shuo Han, Zengyi Gao, Zezhong Ding, Xike Xie, and S Kevin Zhou. Graphinsight: Unlocking insights in large language models for graph structure understanding. *arXiv preprint arXiv:2409.03258*, 2024.
- [88] Yanbin Wei, Shuai Fu, Weisen Jiang, Zejian Zhang, Zhixiong Zeng, Qi Wu, James Kwok, and Yu Zhang. Gita: Graph to visual and textual integration for vision-language graph reasoning. In *The Thirty-eighth Annual Conference on Neural Information Processing Systems*, 2024.
- [89] Eli Chien, Wei-Cheng Chang, Cho-Jui Hsieh, Hsiang-Fu Yu, Jiong Zhang, Olgica Milenkovic, and Inderjit S Dhillon. Node feature extraction by self-supervised multi-scale neighborhood prediction. *ICLR*, 2022.
- [90] Keyu Duan, Qian Liu, Tat-Seng Chua, Shuicheng Yan, Wei Tsang Ooi, Qizhe Xie, and Junxian He. Simteg: A frustratingly simple approach improves textual graph learning. *arXiv preprint arXiv:2308.02565*, 2023.
- [91] Jianan Zhao, Meng Qu, Chaozhuo Li, Hao Yan, Qian Liu, Rui Li, Xing Xie, and Jian Tang. Learning on large-scale text-attributed graphs via variational inference. *ICLR*, 2023.

- [92] Jason Zhu, Yanling Cui, Yuming Liu, Hao Sun, Xue Li, Markus Pelger, Tianqi Yang, Liangjie Zhang, Ruofei Zhang, and Huasha Zhao. Textgnn: Improving text encoder via graph neural network in sponsored search. In *Proceedings of the Web Conference 2021*, pages 2848–2857, 2021.
- [93] Chaozhuo Li, Bochen Pang, Yuming Liu, Hao Sun, Zheng Liu, Xing Xie, Tianqi Yang, Yanling Cui, Liangjie Zhang, and Qi Zhang. Adsgnn: Behavior-graph augmented relevance modeling in sponsored search. In *Proceedings of the 44th international ACM SIGIR conference on research and development in information retrieval*, pages 223–232, 2021.
- [94] Junhan Yang, Zheng Liu, Shitao Xiao, Chaozhuo Li, Defu Lian, Sanjay Agrawal, Amit Singh, Guangzhong Sun, and Xing Xie. Graphformers: Gnn-nested transformers for representation learning on textual graph. *Advances in Neural Information Processing Systems*, 34:28798–28810, 2021.
- [95] Shuxian Bi, Chaozhuo Li, Xiao Han, Zheng Liu, Xing Xie, Haizhen Huang, and Zengxuan Wen. Leveraging bidding graphs for advertiser-aware relevance modeling in sponsored search. In *Findings of the Association for Computational Linguistics: EMNLP 2021*, pages 2215–2224, 2021.
- [96] Bochen Pang, Chaozhuo Li, Yuming Liu, Jianxun Lian, Jianan Zhao, Hao Sun, Weiwei Deng, Xing Xie, and Qi Zhang. Improving relevance modeling via heterogeneous behavior graph learning in bing ads. In *Proceedings of the 28th ACM SIGKDD Conference on Knowledge Discovery and Data Mining*, pages 3713–3721, 2022.
- [97] Aaron Zolnai-Lucas, Jack Boylan, Chris Hokamp, and Parsa Ghaffari. Stage: Simplified text-attributed graph embeddings using pre-trained llms. *arXiv preprint arXiv:2407.12860*, 2024.
- [98] Kaitao Song, Xu Tan, Tao Qin, Jianfeng Lu, and Tie-Yan Liu. MpNet: Masked and permuted pre-training for language understanding. *Advances in neural information processing systems*, 33:16857–16867, 2020.
- [99] Zehan Li, Xin Zhang, Yanzhao Zhang, Dingkun Long, Pengjun Xie, and Meishan Zhang. Towards general text embeddings with multi-stage contrastive learning. *arXiv preprint arXiv:2308.03281*, 2023.
- [100] Gabriel de Souza P Moreira, Radek Osmulski, Mengyao Xu, Ronay Ak, Benedikt Schifferer, and Even Oldridge. Nv-retriever: Improving text embedding models with effective hard-negative mining. *arXiv preprint arXiv:2407.15831*, 2024.
- [101] Hao Yan, Chaozhuo Li, Ruosong Long, Chao Yan, Jianan Zhao, Wenwen Zhuang, Jun Yin, Peiyan Zhang, Weihao Han, Hao Sun, et al. A comprehensive study on text-attributed graphs: Benchmarking and rethinking. *Advances in Neural Information Processing Systems*, 36:17238–17264, 2023.
- [102] Adam Paszke, Sam Gross, Francisco Massa, Adam Lerer, James Bradbury, Gregory Chanan, Trevor Killeen, Zeming Lin, Natalia Gimelshein, Luca Antiga, et al. Pytorch: An imperative style, high-performance deep learning library. *Advances in neural information processing systems*, 32, 2019.
- [103] Matthias Fey and Jan Eric Lenssen. Fast graph representation learning with pytorch geometric. *arXiv preprint arXiv:1903.02428*, 2019.
- [104] T Wolf. Huggingface’s transformers: State-of-the-art natural language processing. *arXiv preprint arXiv:1910.03771*, 2019.
- [105] S. S. SHAPIRO and M. B. WILK. An analysis of variance test for normality (complete samples). *Biometrika*, 52(3-4):591–611, dec 1965.
- [106] Student. The probable error of a mean. *Biometrika*, pages 1–25, 1908.
- [107] Frank Wilcoxon. Individual comparisons by ranking methods. In *Breakthroughs in statistics: Methodology and distribution*, pages 196–202. Springer, 1992.
- [108] Pauli Virtanen, Ralf Gommers, Travis E. Oliphant, Matt Haberland, Tyler Reddy, David Cournapeau, Evgeni Burovski, Pearu Peterson, Warren Weckesser, Jonathan Bright, Stéfan J. van der Walt, Matthew Brett, Joshua Wilson, K. Jarrod Millman, Nikolay Mayorov, Andrew R. J. Nelson, Eric Jones, Robert Kern, Eric Larson, C J Carey, İlhan Polat, Yu Feng, Eric W. Moore, Jake VanderPlas, Denis Laxalde, Josef Perktold, Robert Cimrman, Ian Henriksen, E. A. Quintero, Charles R. Harris, Anne M. Archibald, Antônio H. Ribeiro, Fabian Pedregosa, Paul van Mulbregt, and SciPy 1.0 Contributors. SciPy 1.0: Fundamental Algorithms for Scientific Computing in Python. *Nature Methods*, 17:261–272, 2020.
- [109] Robert J Tibshirani and Bradley Efron. An introduction to the bootstrap. *Monographs on statistics and applied probability*, 57(1):1–436, 1993.
- [110] Hongyun Cai, Vincent W Zheng, and Kevin Chen-Chuan Chang. Active learning for graph embedding. *arXiv preprint arXiv:1705.05085*, 2017.

- [111] Wentao Zhang, Yexin Wang, Zhenbang You, Meng Cao, Ping Huang, Jiulong Shan, Zhi Yang, and Bin Cui. Rim: Reliable influence-based active learning on graphs. *Advances in Neural Information Processing Systems*, 34:27978–27990, 2021.
- [112] Jiaqi Ma, Ziqiao Ma, Joyce Chai, and Qiaozhu Mei. Partition-based active learning for graph neural networks. *arXiv preprint arXiv:2201.09391*, 2022.

6 More Related Works

LLMs for Data Augmentation annotate pseudo-labels via their advanced zero-shot text classification performance. *E.g.*, LLM-GNN [73], Cella [78] and [79] propose heuristics to actively select and annotate pseudo-labels for supervised GNN training. [80] performs knowledge distillation with LLMs as teachers. [81, 82] generate synthetic node text with LLMs. The performance of these methods depend on the capability of LLM, and may still require relatively high annotating and training cost.

LLMs for Graph Property Reasoning focus on reason graph structure properties (e.g., shortest path, node degree, etc) [60, 83, 84, 85]. Representative works include [58, 86, 59, 87, 88].

Tuning LMs/GNNs towards Better Task-Specific Performance aims to push the limits of task-specific performance on TAGs other than generalization. These methods develop novel techniques to optimize LMs or GNNs for pushing the limits of in-domain performance [89, 90, 8, 91, 92, 93, 94, 95, 96, 97, 94].

Text embeddings Generating unified text embeddings is a critical research area with broad applications, including web search and question answering. Numerous text encoders [37, 38, 98] based on pre-trained language models have served as the foundation for various embedding models. Recently, decoder-only LLMs have been widely adopted for text embedding tasks [99, 100] achieving remarkable performance on the Massive Text Embedding Benchmark (MTEB) [63]. This progress stems from LLM2Vec [35], which introduces a novel unsupervised approach to transforming decoder-only LLMs into embedding models, including modifications to enable bidirectional attention. Recent findings [36] suggest that retaining the unidirectional attention mechanism enhances LLM2Vec’s empirical performance.

7 Experiment Details

7.1 Dataset Details

Meta-Data In Table. 3, we show the meta-data of all the eleven datasets used in our experiments.

	Number of Nodes	Number of Edges	Number of Classes	Ground Truth Homophily Ratio
Cora	2708	10556	7	0.809
Citeseer	3186	8450	6	0.764
Pubmed	19717	88648	3	0.792
History	41551	503180	12	0.662
Children	76875	2325044	24	0.464
Sportsfit	173055	3020134	13	0.9
Wikics	11701	431726	10	0.678
Cornell	191	292	5	0.115
Texas	187	310	5	0.067
Wisconsin	265	510	5	0.152
Washington	229	394	5	0.149

Table 3: Meta data of the datasets in this study.

Dataset Split For the datasets (all the homophily graphs) that have been used for study in TSGFM [10], we follow their implementation to perform data pre-processing, obtain raw texts and do data split, the introduction to data source can be found at Appendix.D.2 in their original paper, the code can be found at the link ².

As to the heterophily graphs, the four datasets are originally from [41]. We obtain the raw texts from [101], which can be found from³. As to data split, for zero-shot inference, all the nodes are marked as test data; for few-shot setting, k labeled nodes are randomly sampled per class and the rests are marked as test data. To the best of our knowledge, the four heterophily graph datasets used in this study are the only graphs that provide raw texts feature.

² <https://github.com/CurryTang/TSGFM/tree/master?tab=readme-ov-file>

³ <https://github.com/sktsherlock/TAG-Benchmark/tree/master>

7.2 LLM-BP Implementation Details

Infrastructure and Seeds All the local experiments run on a server with AMD EPYC 7763 64-Core Processor and eight NVIDIA RTX 6000 Ada GPU cards, methods are mainly implemented with PyTorch [102], Torch-Geometric [103] and Huggingface Transformers [104]. To obtain the embeddings, all the encoders that run locally on the server without API calling in this study run with the random seed 42.

Class Embedding

• **Zero-Shot Setting:** We uniformly randomly sample $20c$ nodes per graph, where c denotes the number of classes, we employ GPT-4o [72] to infer their labels. With the predictions from LLMs, the sampled nodes form distinct clusters. For each cluster, we take the top- k (10 in the experiments) nodes whose embedding are closest with the cluster center and calculate their average embedding as the class embedding.

We notice that some works directly feed text descriptions into encoders as class embeddings [56, 10], we find that different encoders can be highly sensitive to variations in text description. Therefore, we adopt the above method to ensure fairness among different encoders.

• **Few-Shot Setting:** We directly take the class embedding as the averaged embeddings of labeled nodes per class.

The Task-Adaptive Encoder: We directly adopt the pre-trained LLM2Vec encoder released by [36], which is based on Mistral7B-v0.1 [75]. We check the pre-training data used in the original paper for aligning LLM decoders with the embedding space, the datasets are mainly for text-retrieval and therefore do not overlap with the TAG datasets adopted in our study. For detailed introduction of the datasets for LLM2Vec pre-training, see Section 4.1 training data in the original paper. The task-adaptive prompting follows the format as:

```

< Instruct >
“Given the {task description}, classify it into one of the following  $k$  classes:
{class labels}
< query >
{raw node texts}.”
< response >

```

, where the {task descriptions} prompts for each dataset is the same as that used for vanilla LLMs, see Table. 11 for details.

Hyper-Parameters for BP algorithm For LLM-BP, we adopt 5 message-passing layers, for its linear approximation form, we use a single layer. The temperature hyper-parameter τ in computing node potential initialization in Eq. (5) is set as 0.025 for LLM-BP and 0.01 for LLM-BP (appr.) across all the datasets. Attached in Table. 4 is the homophily ratio r we used (predicted by GPT-4o-mini [72]).

	Cora	Citeseer	Pubmed	History	Children	Sportsfit	Wikics	Cornell	Texas	Wisconsin	Washington
Ground Truth Homophony Ratio	0.81	0.76	0.79	0.66	0.46	0.90	0.67	0.11	0.06	0.15	0.19
r predicted by GPT-4o-mini	0.70	0.81	0.81	0.73	0.35	0.81	0.52	0.05	0.04	0.06	0.02

Table 4: r predicted by GPT-4o-mini, that is used in all the experiments in this study.

7.3 Baseline Implementation Details

• **Vanilla Encoders** Vanilla encoders like SBert [37], Roberta [38] and text-embedding-3-large [71] directly encode the raw text of the nodes. LLM2Vec uses the prompts:

$$\langle \text{Instruct} \rangle \{ \text{task_description} \} \langle \text{query} \rangle X_i \langle \text{response} \rangle. \quad (8)$$

, where the {task_description} for each dataset is provided in Appendix. 10.1.

• **Vanilla LLMs** Prompts for GPT-4o and GPT-3.5-turbo adopts the format as follows:

```

“role”: “system”
“content”: “You are a chatbot who is an expert in text classification”

```

“role”: “user”
 “content”: “We have {task description} from the following k categories: {class labels}
 The text is as follows:
 {raw node text}
 Please tell which category the text belongs to:”

The {task description} for the vanilla LLMs for each class is provided in Appendix. 10.2.

• Tuning LM/GNNs We adopt the pre-trained UniGLM [19] released by the official implementation, which adopts Bert as the encoder, for direct inference. For ZeroG [18], we re-implement the method and train it on ogbn-arxiv [53] for fair comparison with other baselines.

As to GNNs tuning methods, we pre-train GraphMAE [20] and DGI [21] on ogbn-arxiv [53], where the input for both models are from SBert [37], and we follow in implementation in TSGFM [10] benchmark.

• Multi-Task GFMs OFA [55] is trained on ogbn-arxiv [53]. As to GOFA, we directly adopt the model after pre-training [76, 77] and instruct fine-tuning on ogbn-arxiv [53] provided by the authors due to the huge pre-training cost, the zero-shot inference scheme also follows their original implementation.

• LLMs with Graph Adapters Both LLaGA [26] and GraphGPT [27] are trained on ogbn-arxiv [53], we follow the hyper-parameter setting in their original implementation.

8 Detailed Derivations

8.1 Derivation for Eq. (4)

In a node classification task, given a node i , our goal is to minimize the mean-square error (MSE) in predicting the node label under the observations \mathbf{X} :

$$\min \text{MSE}(\hat{y}_i) = \mathbb{E}[(y_i - \hat{y}_i)^2 \mid \mathbf{X}]. \quad (9)$$

The optimal solution \hat{y}_i is then given by:

$$\hat{y}_i = \sum_{y_i} y_i p(y_i \mid \mathbf{X}), \quad (10)$$

where the posterior marginal $p(y_i \mid \mathbf{X})$ is computed as:

$$p(y_i \mid \mathbf{X}) = \sum_{Y \setminus i} \mathbb{P}(Y \mid \mathbf{X}). \quad (11)$$

Factorized Posterior under an MRF. Assuming a Markov Random Field (MRF) over a graph $\mathcal{G} = (\mathcal{V}, \mathcal{E})$, the posterior distribution factors as:

$$\mathbb{P}_{\mathcal{G}}(Y \mid \mathbf{X}) \propto \prod_{i \in \mathcal{V}} \varphi_{X_i}(y_i) \prod_{(i,j) \in \mathcal{E}} \psi_{ij}(y_i, y_j), \quad (12)$$

where the node potential is defined as $\varphi_{X_i}(y_i) = \varphi_{y_i}(X_i) \phi_i(y_i)$.

General Message-Passing Framework. To compute the marginal $p(y_i \mid \mathbf{X})$, the loopy belief propagation (LBP) algorithm iteratively updates messages between nodes. The general message update rule from node i to node j at iteration k is:

$$m_{i \rightarrow j}^{(k)}(y_j) = \alpha_{i \rightarrow j} \sum_{y_i} \left[\varphi_{X_i}(y_i) \psi_{ij}(y_i, y_j) \prod_{\ell \in \mathcal{N}(i) \setminus j} m_{\ell \rightarrow i}^{(k-1)}(y_i) \right], \quad (13)$$

where $\alpha_{i \rightarrow j}$ is a normalization constant ensuring the message sums to 1.

Node Belief Updates. The node belief $p_i^{(k)}(y_i)$ at iteration k is obtained by combining the node potential with incoming messages from all neighbors:

$$p_i^{(k)}(y_i) = \varphi_{X_i}(y_i) \prod_{\ell \in \mathcal{N}(i)} m_{\ell \rightarrow i}^{(k)}(y_i). \quad (14)$$

Reformulating the Messages. Substituting Eq. (14) into Eq. (13) simplifies the message-passing equation. The message from node i to node j at iteration k can be rewritten as:

$$m_{i \rightarrow j}^{(k)}(y_j) = \alpha_{i \rightarrow j} \sum_{y_i} \psi_{ij}(y_i, y_j) \frac{p_i^{(k)}(y_i)}{m_{j \rightarrow i}^{(k-1)}(y_i)}. \quad (15)$$

This reformulation prevents double-counting the contribution of node j to node i in the previous iteration.

Log-Space Stability. To avoid numerical underflow, the log-space version of the message update is commonly used:

$$\log m_{i \rightarrow j}^{(k)}(y_j) = \text{LSE}_{y_i} \left[\log \psi_{ij}(y_i, y_j) + \log p_i^{(k)}(y_i) - \log m_{j \rightarrow i}^{(k-1)}(y_i) \right], \quad (16)$$

where $\text{LSE}(\cdot) \equiv \log \sum \exp(\cdot)$.

Summary. By iteratively applying these message updates and node belief calculations, LBP provides an approximation for the posterior marginal $p(y_i | \mathbf{X})$. The final prediction \hat{y}_i under the MMSE criterion is:

$$\hat{y}_i = \sum_{y_i} y_i p_i^{(k)}(y_i). \quad (17)$$

This completes the derivation of the message-passing update in Eq. (4).

9 More Experiment Results

9.1 Significance Test of Effectiveness of Task-Adaptive Encoding

		Cora	Citeseer	Pubmed	History	Children	Sportsfit	Wikies	Cornell	Texas	Wisconsin	Washington
Task-Adaptive Encoding vs. Vanilla LLM2Vec	90% CI low, high	0.7% 1.3%	-0.2% 1.3%	1.3% 2.3%	3.2% 5.2%	3.3% 3.7%	1.0% 2.6%	1.0% 1.8%	4.0% 4.9%	1.5% 2.7%	0.1% 0.8%	-0.2% 0.5%
	P value	1e-8	0.38	1e-10	1e-9	3e-59	1e-4	3e-8	7e-18	5e-8	1e-3	0.82
Task-Adaptive Encoding vs. Text-Embedding-3-Large	90% CI low, high	-0.3% -0.2%	0.5% 1.0%	-0.3% 1.0%	6.9% 9.1%	4.1% 4.4%	0.7% 2.8%	1.1% 2.0%	3.1% 4.1%	3.1% 4.7%	0.1% 1.2%	-0.04% -0.1%
	P value	6e-27	8e-7	0.51	7e-21	5e-59	0.03	1e-9	2e-25	1e-9	0.07	1e-13

Table 5: Lower and upper bound of improvement (\uparrow) in accuracy of task-adaptive encoding over baselines with 90% confidence interval, with significance level p (\downarrow).

We conduct significance test on the improvment of task-adaptive encoding over vanilla LLM2Vec [36] and Text-Embedding-3-Large [71] under the zero-shot setting, with results shown in Table. 5. We replicate experiment for 100 times with random seeds from 42 to 141 and obtain classification accuracy of each method. To check normality, we first apply Shapiro-Wilk test [105]. If the data follows a normal distribution, we perform a Paired-t test [106]; otherwise, we use Wilcoxon Signed-Rank test [107], with packages from SciPy [108]. The lower and upper bounds under 90% confidence interval are estimated with bootstrap algorithm [109] to sample 10,000 times. Task-adaptive encoding show statistically significant improvement over vanilla LLM2Vec in 9 out of 11 dataset and outperforms Text-Embedding-3-Large in 8 out of 11 datasets (bolded in the table).

9.2 LLM Agents' Prediction on Homophily Ratio r

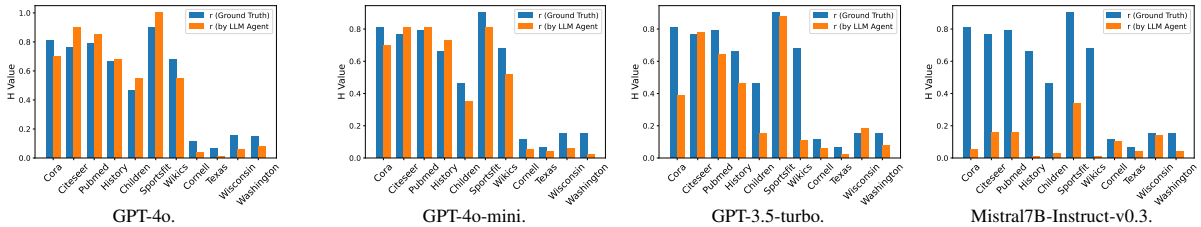


Figure 7: LLM agents' performance on predicting the homophily constant r .

More prediction performance of GPT-4o, GPT-3.5-turbo and Mistral7b-Instruct-v3 are shown in Fig. 7.

	Cora	Citeseer	Pubmed	Wikics
DA-AGE-W	74.96	58.41	65.85	59.13
DA-RIM-W	74.73	60.80	77.94	68.22
DA-GraphPart-W	68.61	68.82	79.89	67.13
LLM-BP	72.59	69.51	75.55	67.75
LLM-BP (app.)	71.41	68.66	76.81	67.96

Table 6: Accuracy compared with LLM-GNN, where ‘DA’ denotes the ‘C-Density’ methods proposed in [73], ‘-W’ refers to the weighted cross-entropy loss function used for training, AGE [110], RIM [111], GraphPart [112] are different graph active learning baselines used in the original paper.

	Cora	Pubmed	History	Children
TEA-GLM	20.2	84.8	52.8	27.1
LLM-BP	72.59	75.55	59.86	24.81
LLM-BP (app.)	71.41	76.81	59.49	29.4

Table 7: Accuracy compared with TEA-GLM [29].

9.3 Zero-Shot Comparison with LLM-GNN [73] and TEA-GLM [29]

Here we present the comparison with LLM-GNN [73] in Table. 6. We compare with three different graph active learning heuristics from their original paper. Our training-free methods, LLM-BP and LLM-BP (app.) achieves top performance on Citeseer and Wikics, while performs comparably with the baselines in Cora and Pubmed. Note that the results of LLM-GNN are from Table. 2 in the original paper.

The comparison with TEA-GLM is shown in Table. 7. Results of TEA-GLM are from Table.1 in their original paper.

9.4 Experiment Results in Few-Shot Setting

We use 10 different random seeds from 42 to 52 to sample the k -shot labeled nodes from training dataset, and report the average accuracy and macro $F1$ score with standard variance. Results are shown in Table. 8. Across all the k s, our LLM-BP achieves the top ranking performance across all the eleven datasets, exhibiting similar insights with the zero-shot setting.

		Cora		Citeseer		Pubmed		History		Children		Sportsf		Wikics		Cornell		Texas		Wisconsin		Washington		Avg. Rank	
		Acc	F1	Acc	F1	Acc	F1	Acc	F1	Acc	F1	Acc	F1	Acc	F1	Acc	F1	Acc	F1	Acc	F1	Acc	F1	Acc	F1
10-shot																									
SBert	Raw	42.8±5.2	42.1±5.7	38.8±6.6	52.2±6.7	51.1±6.6	30.6±7.3	14.9±2.5	10.5±3.2	9.1±1.7	17.8±4.4	17.2±3.0	34.6±3.2	31.0±3.1	40.4±9.1	32.3±6.9	26.3±9.4	23.5±6.0	47.0±7.7	35.1±5.0	36.0±12.8	27.6±8.4	9.9	10.7	
SBert	BP	43.9±5.1	43.0±5.6	43.8±8.1	39.9±7.0	53.6±6.8	52.2±6.7	33.0±8.2	15.5±2.6	8.8±2.7	8.4±1.4	18.7±5.1	18.3±3.5	32.0±3.5	41.3±8.9	33.4±6.5	27.9±8.1	25.6±5.7	47.8±8.4	35.8±5.2	35.9±11.4	27.9±7.3	8.5	8.6	
SBert	BP (app.)	43.1±4.9	42.4±5.4	42.8±7.7	39.1±6.6	52.5±6.7	51.3±6.6	31.2±7.6	15.1±2.6	10.6±3.3	9.2±1.6	18.0±4.5	17.4±3.1	35.2±3.3	41.3±3.2	40.9±9.0	32.9±6.9	26.7±9.1	24.1±5.9	35.2±5.0	36.0±12.3	27.8±8.1	8.9	9.5	
TE-3-Large	Raw	47.2±5.4	46.3±5.7	40.2±6.3	37.0±5.5	55.2±7.3	52.8±7.2	22.9±7.1	12.5±1.9	13.3±2.7	12.0±1.4	31.1±6.6	30.6±4.3	40.3±4.6	36.4±3.4	55.4±8.4	46.5±7.0	50.8±7.7	42.5±6.4	58.6±5.2	47.8±4.3	44.2±16.9	36.1±10.6	7.2	7.1
TE-3-Large	BP	49.1±5.3	48.0±5.5	41.6±7.0	38.0±6.1	53.8±8.6	52.7±8.5	24.1±8.0	13.1±2.1	12.0±1.3	10.8±1.3	34.7±7.4	32.1±4.8	42.4±5.0	38.0±3.7	59.6±6.8	50.7±6.6	52.9±8.2	44.5±6.5	59.8±5.6	49.0±4.5	45.5±15.8	37.9±10.4	5.2	5.1
TE-3-Large	BP (app.)	48.4±5.2	47.4±5.6	40.7±6.6	37.4±5.7	55.4±7.7	52.8±7.5	23.3±7.4	12.7±2.0	13.4±2.7	12.2±1.4	33.5±6.8	30.9±4.9	41.3±4.8	37.3±3.5	57.0±7.3	47.7±6.8	51.8±8.0	43.4±6.6	59.0±5.0	48.5±4.5	44.3±16.6	36.3±10.2	6.1	6.0
LLM2Vec	Raw	39.8±6.6	38.0±6.9	47.9±9.5	42.2±7.7	54.9±7.7	52.5±7.9	24.2±12.9	12.8±3.6	10.0±1.4	8.8±1.3	27.6±5.6	26.1±4.9	33.9±4.1	31.3±3.8	50.1±12.5	40.8±8.8	50.9±12.0	40.9±6.5	61.1±7.7	48.7±5.6	50.0±20.8	36.5±10.4	8.5	8.7
LLM2Vec	BP	40.5±6.7	38.5±7.0	48.9±10.7	42.7±8.6	54.6±9.1	51.5±9.6	25.7±14.6	13.4±4.1	9.4±1.3	8.8±1.1	29.2±6.3	27.8±5.5	34.3±4.5	31.7±4.2	53.0±9.9	43.8±6.6	52.9±11.2	42.5±6.7	64.2±7.4	51.9±4.5	49.4±18.3	38.0±9.4	7.4	7.2
LLM2Vec	BP (app.)	40.3±6.6	38.4±7.0	48.6±10.0	42.6±8.1	55.2±8.0	52.8±8.2	25.0±13.7	13.3±3.8	10.1±1.5	10.0±1.4	28.0±5.8	26.7±5.1	34.6±4.6	31.9±4.1	51.7±11.2	42.3±7.4	52.1±11.3	42.0±6.2	62.5±7.2	49.8±4.7	49.7±20.2	36.8±10.0	7.4	7.1
LLM-BP (ours)	Raw	43.5±5.9	42.4±6.1	53.0±8.3	47.3±6.6	57.0±1.1	54.8±8.8	28.7±1.4	17.2±2.7	13.4±3.1	10.4±1.3	36.4±7.7	35.3±7.3	38.4±7.8	42.5±4.4	57.5±12.4	47.9±10.3	60.0±7.2	48.7±5.7	69.5±10.6	54.5±6.6	53.4±19.4	39.0±10.1	3.8	3.5
LLM-BP (ours)	BP	46.3±6.8	44.4±7.2	54.4±8.9	48.4±7.1	58.2±8.1	54.2±10.5	30.1±12.9	17.7±4.0	12.5±2.5	13.2±2.0	37.7±8.2	36.6±7.7	39.3±9.2	35.7±6.5	64.8±7.4	54.2±7.6	63.0±11.3	51.3±6.6	73.6±8.8	59.3±6.4	53.6±17.6	42.3±10.0	2.3	2.0
LLM-BP (ours)	BP (app.)	44.7±6.4	43.5±6.4	53.7±8.5	47.9±6.8	57.7±7.4	54.5±9.2	29.5±12.2	17.3±3.2	14.8±2.4	16.9±7.9	35.8±7.3	39.3±8.5	36.0±6.1	61.0±10.8	50.8±9.7	62.1±11.9	50.5±6.5	71.3±9.9	56.6±6.3	54.1±19.1	40.8±10.6	2.7	2.4	
3-shot																									
SBert	Raw	57.6±5.2	56.8±5.3	57.3±4.0	53.2±3.7	62.1±5.1	62.7±4.7	42.8±2.2	21.9±2.4	13.6±2.2	13.1±0.9	31.7±3.8	29.3±2.8	47.2±4.4	44.4±3.8	51.8±5.0	41.4±4.8	49.5±7.3	36.1±4.5	54.9±6.1	43.1±4.7	49.4±11.2	39.1±6.3	11.1	11.4
SBert	BP	58.7±5.3	57.9±5.3	58.6±4.5	54.3±4.2	63.7±6.1	64.3±5.6	47.0±2.4	23.4±2.4	12.5±1.9	11.8±0.8	35.1±4.4	32.6±3.1	49.5±4.5	46.4±4.0	52.2±4.7	42.4±4.6	48.9±6.9	36.6±4.7	55.0±5.9	43.4±4.8	50.2±9.5	39.9±5.8	9.6	9.5
SBert	BP (app.)	58.4±5.1	57.6±5.2	57.7±4.2	53.6±3.9	62.5±5.1	63.1±4.7	43.8±2.2	23.2±2.5	13.7±2.2	13.3±1.0	32.3±3.9	29.9±2.8	48.2±4.5	45.4±3.9	51.6±4.5	41.5±4.6	49.7±7.3	36.4±4.4	54.7±5.7	42.9±4.2	49.8±10.3	39.4±5.9	10.4	10.5
TE-3-Large	Raw	64.1±5.6	62.8±4.8	55.1±4.3	51.8±3.9	70.6±4.8	69.9±4.9	38.9±4.7	21.0±1.9	18.0±2.5	17.9±1.6	54.0±4.6	49.9±2.8	54.8±4.3	51.4±4.0	72.8±3.3	63.2±2.2	77.9±7.7	67.8±1.6	69.8±8.1	58.9±6.2	61.1±13.0	49.3±6.5	7.5	7.9
TE-3-Large	BP	66.3±5.8	64.8±4.9	57.5±4.8	53.8±4.3	72.4±5.6	71.6±5.7	42.4±6.0	22.3±2.3	16.2±2.1	15.9±1.3	56.3±5.0	52.2±3.1	57.0±4.4	53.5±4.2	73.3±3.7	63.6±2.9	79.5±7.3	69.8±12.2	70.9±8.3	60.1±6.2	63.8±9.5	51.4±5.0	5.5	5.3
TE-3-Large	BP (app.)	65.6±5.8	64.1±4.9	56.0±4.4	52.6±4.0	71.1±5.0	70.4±5.1	40.1±5.2	21.5±2.0	18.3±2.5	18.2±1.6	54.7±4.7	50.6±2.9	56.2±4.4	52.8±4.1	73.2±3.5	63.6±2.9	78.7±7.5	68.8±11.8	70.5±8.4	59.4±6.3	62.0±12.0	51.0±5.8	6.3	6.5
LLM2Vec	Raw	56.9±4.9	56.5±4.9	62.3±4.2	58.1±3.7	66.6±6.4	66.9±5.9	45.4±9.2	24.2±3.4	18.1±3.4	17.8±1.1	49.5±3.6	46.9±2.2	51.7±5.1	49.5±5.2	72.6±5.4	61.9±6.9	75.0±7.1	71.5±8.3	70.7±6.1	59.5±4.7	63.3±10.2	49.6±3.9	8.2	8.0
LLM2Vec	BP	59.6±5.3	59.0±5.3	64.6±4.5	59.9±3.9	67.3±7.5	67.4±6.7	48.9±10.5	25.8±4.0	16.4±2.8	15.6±1.0	52.8±3.9	50.1±2.5	53.9±6.0	51.5±5.7	74.1±5.2	64.2±6.5	79.6±4.6	74.5±8.1	72.6±5.0	60.7±4.0	65.0±10.0	51.7±4.1	5.5	5.5
LLM2Vec	BP (app.)	59.2±5.0	58.7±4.9	63.7±4.3	59.2±3.7	67.1±6.6	67.4±6.0	47.4±9.8	25.4±3.7	18.7±3.7	18.3±1.1	50.9±3.7	48.2±2.2	54.0±5.5	51.8±5.3	74.1±5.1	64.0±6.4	77.6±5.2	73.2±7.4	72.2±5.6	60.6±4.6	64.6±10.1	50.8±4.1	6.1	5.9
LLM-BP (ours)	Raw	60.0±4.0	59.2±3.9	64.6±4.4	60.3±3.6	68.7±5.2	69.0±4.8	59.8±6.0	32.2±3.0	22.3±3.3	22.3±1.5	58.2±4.0	55.7±2.6	55.1±4.9	53.5±4.6	79.9±3.8	72.2±5.7	82.5±5.4	79.0±6.2	83.0±4.0	72.3±4.6	71.4±12.5	58.3±6.0	3.6	3.5
LLM-BP (ours)	BP	69.5±3	68.3±3.3	67.4±5.8	63.3±5.1	69.7±6.2	69.7±5.8	62.8±6.1	33.4±3.2	24.3±2.2	23.5±0.9	66.6±5.6	63.6±2.4	65.2±3.7	63.1±3.7	83.3±3.1	77.6±4.8	88.2±2.8	86.3±2.6	88.4±2.5	73.3±4.2	71.9±10.6	60.1±5.7	1.9	1.7
LLM-BP (ours)	BP (app.)	61.7±4.2	60.2±3.8	66.7±5.8	62.8±5.3	73.9±6.2	74.1±5.6	64.9±4.7	36.3±3.4	26.9±2.7	27.0±1.1	65.5±5.6	62.5±4.2	64.6±3.4	62.8±3.5	83.6±2.9	77.6±4.4	89.3±2.7	86.4±2.8	78.2±6.9	74.7±4.9	64.8±5.4	2.4	2.4	
1-shot																									
SBert	Raw	68.3±3.1	68.5±3.1	67.0±2.0	63.0±1.8	68.9±4.1	69.3±4.6	57.3±2.7	31.2±0.9	20.1±2.8	19.7±0.9	40.3±3.2	33.5±2.0	59.8±1.9	58.1±1.6	71.2±2.9	68.1±4.9	60.5±3.7	42.2±6.6	66.1±3.4	49.4±3.8	62.8±4.1	46.3±3.1	11.3	11.2
SBert	BP	69.6±3.2	69.2±2.9	68.3±1.9	64.1±1.7	70.5±4.0	70.8±4.0	61.6±2.9	33.2±1.2	18.0±1.4	17.3±0.8	43.4±3.6	39.3±2.2	60.8±1.9	60.2±0.7	74.8±2.7	68.0±3.3	60.0±3.3	46.6±5.0	66.2±4.0	49.3±3.8	58.5±4.7	46.3±3.1	9.8	10.1
SBert	BP (app.)	70.3±3.2	69.8±3.1	67.5±1.8	64.1±1.7	69.3±4.3	69.7±4.8	58.5±2.8	31.0±1.0	20.6±1.9	20.1±1.0	47.8±4.4	44.6±2.0	60.8±1.9	59.5±1.8	80.2±2.6	68.7±4.6	60.4±3.6	46.6±6.2	66.4±3.4	49.6±4.1	62.0±4.1	45.8±3.7	10.4	10.5
TE-3-Large	Raw	74.9±1.2	73.7±1.4	65.7±1.8	61.9±1.5	78.3±1.2	78.1±4.0	59.8±6.5	33.0±1.2	22.7±2.3	22.6±1.6	61.3±3.8	61.1±2.1	68.8±1.9	66.6±1.7	82.1±2.1	71.6±3.1	86.3±2.9	74.9±2.9	81.8±3.5	68.3±6.5	74.7±4.2	65.1±4.5	7.5	7.6
TE-3-Large	BP	76.6±1.3	75.2±1.5	68.3±2.0	64.0±1.7	79.1±4.4	78.7±4.3	63.9±6.7	34.8±2.4	20.9±1.7	23.4±1.0	70.0±4.1	65.2±2.1	71.3±2.0	68.8±1.8	80.5±2.7	72.3±4.1	87.2±2.6	85.4±2.8	81.9±2.9	68.7±5.2	73.7±3.9	60.7±3.1	5.5	5.5
TE-3-Large	BP (app.)	76.5±1.3	75.1±1.5	68.3±2.0	64.0±1.7	79.1±4.4	78.7±4.3	63.9±6.7	34.8±2.4	20.9±1.7	23.4±1.0	70.0±4.1	65.2±2.1	71.3±2.0	68.8±1.8	80.5±2.7	72.3±4.1	87.2±2.6	85.4±2.8	81.9±2.9	68.7±5.2	73.7±3.9	60.7±3.1	5.5	5.5
LLM2Vec	Raw	68.1±2.7	66.9±2.8	60.8±2.8	56.2±2.6	72.9±4.2	72.3±3.9	65.9±4.2	37.1±1.8	27.2±2.8	27.0±1.3	63.0±4.3	60.7±1.6	68.6±2.6	66.7±2.4	80.6±3.6	72.9±4.3	85.9±3.0	82.4±2.8	81.5±4.7	69.0±5.1	81.6±4.5	61.4±5.9	7.5	7.7
LLM2Vec	BP	70.4±3.0	69.3±3.3	70.6±2.9	66.5±2.7	73.9±4.1	75.0±3.8	69.9±4.2	39.6±2.4	24.6±2.5	23.2±1.1	62.4±3.6	60.5±2.1	71.7±2.6	68.8±2.4	80.9±3.1	73.5±4.2	87.2±3.0	84.9±2.8	85.9±2.4	70.3±4.3	80.5±4.4	63.0±5.3	5.2	5.2
LLM2Vec	BP (app.)	70.0±3.0	68.8±3.1	69.5±2.8	65.7±2.7	74.5±4.2	73.8±4.0	68.2±4.2	39.6±2.4	23.3±1.3	27.8±1.3	62.9±3.5	62.2±1.7	71.2±2.5	69.1±2.4	81.5±2.9	73.6±2.9	86.2±3.3	86.0±1.8	70.6±4.1	74.7±4.3	62.9±5.3	5.8	5.7	
LLM-BP (ours)	Raw	70.4±3.2	69.3±3.4	69.1±2.6	65.5±2.2	74.3±4.3	74.5±4.2	72.3±3.1	43.5±2.1	30.8±2.0	30.4±0.9	68.9±3.6	65.2±1.7	74.7±2.2	73.6±2.3	85.9±3.2	80.8±4.2	88.2±3.6	86.2±3.6	80.7±4.1	77.8±7.5	85.9±2.7	68.8±3.7	3.6	3.6
LLM-BP (ours)	BP	70.7±3.2	69.3±3.4	69.1±2.6	65.5±2.2	74.3±4.3	74.5±4.2	72.3±3.1	43.5±2.1	30.8±2.0	30.4±0.9	68.9±3.6	65.2±1.7	74.7±2.2	73.6±2.3	85.9±3.2	80.8±4.2	88.2±3.6	86.2±3.6	80.7±4.1	77.8±7.5	85.9±2.7	68.8±3.7	3.6	3.6
LLM-BP (ours)	BP (app.)	71.9±3.3	70.6±3.7	70.4±2.6	67.1±2.1	74.8±4.4	75.0±4.2	73.6±3.0	44.6±2.1	31.2±1.0	30.8±1.0	69.7±3.5	66.5±1.7	74.6±2.2	71.6±2.1	86.8±2.9	81.0±3.8	90.7±1.9	88.1±3.0	91.7±1.7	78.8±5.2	85.9±2.3	63.8±4.0	2.5	2.3

9.5 Zero-Shot Link Prediction Results

	Citation Graph			E-Commerce & Knowledge Graph			
	Cora	Citeseer	Pubmed	History	Children	Sportsfit	Wikics
OFA	0.492	–	0.481	0.431	0.484	0.517	–
LLaGA	0.527	–	0.543	0.515	0.500	0.502	–
GraphGPT	0.520	–	0.569	0.449	0.422	0.597	–
TEA-GLM	0.586	–	0.689	0.579	0.571	0.553	–
SBert	0.979±0.033	0.990±0.001	0.979±0.003	0.985±0.002	0.972±0.030	0.975±0.003	0.972±0.003
Text-Embedding-3-Large	0.975±0.003	0.989±0.002	0.979±0.003	0.985±0.001	0.980±0.002	0.987±0.001	0.977±0.002
LLM2Vec	0.966±0.004	0.982±0.002	0.970±0.003	0.971±0.002	0.973±0.003	0.975±0.002	0.978±0.003

Table 9: Performance on zero-shot link prediction tasks (AUC). Results of baselines are from [29].

For each dataset, We randomly sample & remove 1000 edges and 1000 node pairs from the graph as testing data. A straightforward approach is to compare the cosine similarity between node embeddings to determine the presence of a link. Specifically, we aggregate embeddings for 3 layers on the incomplete graph and compute the cosine similarity between node representations, achieving better zero-shot performance than LLMs-with-Graph-Adapters methods [29, 26, 27], as shown in Table. 9. Note that the performance in the table refers to LLM-with-Graph-Adapters that have only been trained on other tasks and never on link prediction tasks.

We leave the design of task-adaptive embeddings and generalized graph structural utilization for link prediction as future work, including task-adaptive encoding prompts.

10 Prompts

10.1 Task Description for Vanilla LLM2Vec without Class Information

Table. 10 shows the task description for vanilla LLM2Vec encoder across all the datasets.

Dataset	Task Description
Cora	Encode the text of machine learning papers:
Citeseer	Encode the description or opening text of scientific publications:
Pubmed	Encode the title and abstract of scientific publications:
History	Encode the description or title of the book:
Children	Encode the description or title of the child literature:
Sportsfit	Encode the title of a good in sports & fitness:
Wikics	Encode the entry and content of wikipedia:
Cornell	Encode the webpage text:
Texas	Encode the webpage text:
Wisconsin	Encode the webpage text:
Washington	Encode the webpage text:

Table 10: {Task description} for vanilla LLM2Vec [36] encoder. See Eq. 8 for detailed prompting format.

10.2 Prompts for Vanilla LLMs

Table. 11 shows tha task description for vanilla LLM decoders.

Dataset	Task Description
Cora	opening text of machine learning papers
Citeseer	description or opening text of scientific publications
Pubmed	title and abstract of scientific publications
History	description or title of the book
Children	description or title of the child literature
Sportsfit	the title of a good in sports & fitness
Wikics	entry and content of wikipedia
Cornell	webpage text
Texas	webpage text
Wisconsin	webpage text
Washington	webpage text

Table 11: {Task description} in the prompts for both vanilla LLM decoders (See Section. 7.3) and task-adaptive encoder (See Section. 7.2).